공학박사 학위논문

A Study on the Wearable and Cuffless Continuous Blood Pressure Monitoring System

커프리스 방식의 착용형 연속 혈압 모니터링 시스템에 관한 연구

2019 년 2 월

서울대학교 대학원
협동과정 바이오엔지니어링 전공
박 종 현

A Study on the Wearable and Cuffless Continuous Blood Pressure Monitoring System

지도교수 김 희 찬

이 논문을 공학박사 학위논문으로 제출함
2018 년 10 월

서울대학교 대학원
협동과정 바이오엔지니어링 전공
박 종 현

박종현의 공학박사 학위논문을 인준함
2018 년 12 월

위 원 장	이 정 찬	(인)
부위원장	김 희 찬	(인)
위 원	최 영 빈	(인)
위 원	구 윤 서	(인)
위 원	노 승 우	(인)

Ph. D. Dissertation

A Study on the Wearable and Cuffless Continuous Blood Pressure Monitoring System

BY

JONG HYUN PARK

FEBRUARY 2019

INTERDISCIPLINARY PROGRAM IN BIOENGINEERING

THE GRADUATE SCHOOL

SEOUL NATIONAL UNIVERSITY

A Study on the Wearable and Cuffless Continuous Blood Pressure Monitoring System

BY
JONG HYUN PARK

INTERDISCIPLINARY PROGRAM IN
BIOENGINEERING
THE GRADUATE SCHOOL
SEOUL NATIONAL UNIVERSITY

THIS DISSERTATION IS APPROVED FOR
THE DEGREE OF DOCTOR OF PHILOSOPHY

DECEMBER 2018

Approved by Thesis Committee:

Professor _____ Chairman
Jung Chan Lee

Professor _____ Vice chairman
Hee Chan Kim

Professor _____ Member
Young Bin Choy

Professor _____ Member
Yunseo Ku

Professor _____ Member
Seungwoo Noh

ABSTRACT

A Study on the Wearable and Cuffless Continuous Blood Pressure Monitoring System

Jonghyun Park
Interdisciplinary Program in Bioengineering
The Graduate School
Seoul National University

Continuous blood pressure (BP) monitoring is needed in daily life to enable early detection of hypertension and improve control of BP for hypertensive patients. Although the pulse transit time (PTT)-based BP estimation represents one of most promising approaches, its use in daily life is limited owing to the requirement of multi systems to measure PTT, and its performance in systolic blood pressure (SBP) estimation is not yet satisfactory.

The first goal of this study is to develop a wearable system providing convenient measurement of the PTT, which facilitates continuous BP monitoring based on PTT in daily life. A single chest-worn device was developed measuring a

photoplethysmogram (PPG) and a seismocardiogram (SCG) simultaneously, thereby obtaining PTT by using the SCG as timing reference of the aortic valve opening and the PPG as timing reference of pulse arrival. The presented device was designed to be compact and convenient to use, and to last for 24h by reducing power consumption of the system. The consistency of BP related parameters extracted from the system including PTT between repetitive measurements was verified by an intra-class correlation analysis, and it was over 0.8 for all parameters. In addition, the use of SCG as timing reference of the aortic valve opening was verified by comparing it with an impedance cardiogram ($r = 0.79 \pm 0.14$).

Secondly, the algorithm improving the performance of the SBP estimation was developed by using the presented system. A multivariate model using SCG amplitude (SA) in conjunction with PTT was proposed for SBP estimation, and was compared with conventional models using only PTT or pulse arrival time (PAT) in various interventions inducing BP changes. Furthermore, we validated the proposed model against the general population with a simple calibration process and verified its potential for daily use. The results suggested that (1) the proposed model, which

employed SA in conjunction with PTT for SBP estimation, outperformed the conventional univariate model using PTT or PAT (the mean absolute errors were of 4.57, 6.01, and 6.11 for the proposed, PTT, and PAT models, respectively); (2) for practical use, the proposed model showed potential to be generalized with a simple calibration; and (3) the proposed model and system demonstrated the potential for continuous BP monitoring in daily life without any intervention of users or regulations.

In conclusion, the presented system provides an improved performance of continuous BP monitoring in daily life by using a combination of PTT and SA with a convenient and compact single chest-worn device, and thus, it can contribute to mobile healthcare services.

Keywords: Blood pressure, Continuous blood pressure monitoring, Mobile healthcare, Wearable device, Pulse transit time, Photoplethysmogram, Seismocardiogram.

Student number: 2015-31046

CONTENTS

LIST OF TABLES

LIST OF FIGURES

LIST OF ABBREVIATIONS

BP	Blood Pressure
SBP	Systolic Blood Pressure
DBP	Diastolic Blood Pressure
MBP	Mean Blood Pressure
PP	Pulse pressure
ABPM	Ambulatory Blood Pressure Monitoring
PTT	Pulse Transit Time
PAT	Pulse arrival Time
PEP	Pre-ejection Periods
SA	SCG amplitude
HR	Heart Rate
PWV	Pulse Wave Velocity
PPG	Photoplethysmogram
ECG	Electrocardiogram
SCG	Seismocardiogram
ICG	Impedance-cardiogram
BCG	Ballistocardiogram
ADC	Analog-to-digital converter
DAC	Digital-to-analog converter
MCU	Micro control unit

TIA	Trans-impedance amplifier
PCB	Printed circuit board
GUI	Graphical User Interface
AO	Aortic Valve Opening
IT	Intersecting tangent
LV	Left ventricle
SV	Stroke Volume
HDU	Head-Down/Up
CO	Cardiac Output
TPR	Total Peripheral Resistance
MAD	Mean Absolute Difference
AAMI	Association for the Advancement of Medical Instrumentation
BSH	British Society of Hypertension
LVET	Left Ventricle Ejection Time

CHAPTER 1

General Introduction

1.1. BLOOD PRESSURE

Blood pressure (BP) is the pressure of circulating blood on the vessel wall. As the circulation of the blood is not constant but variable owing to the pulsatile function of the heart, BP is a function of time. BP is normally expressed by two values, the systolic blood pressure (SBP) and diastolic blood pressure (DBP), which are the maximum and minimum blood pressures during one cardiac cycle, respectively, and it is measured by various methods.

The first measurement of BP was performed by Hales by inserting a tube into an artery, and it is regarded as the most direct and precise measurement method until now, albeit it is invasive (1). As a non-invasive means, the auscultatory method is widely accepted as a standard clinical method, which measures BP by detecting Korotkoff sounds when occluding and releasing an artery with an inflating and deflating cuff (2). Similarly, the oscillometric method is the most popular method, widely used in homes and clinics, which measures BP by automatically analyzing the oscillation in an artery when occluding and releasing it by a cuff, as in the auscultatory method (3). The volume clamping

method is also available and often used for research purposes, as it provides instantaneous BP by using a cuff that continuously varies its pressure via a fast servo-control system (4).

BP is one of the vital signs, along with the heart rate (HR), respiratory rate, and body temperature, as the BP value can represent the condition of the hemodynamic system of the body, and further indicate the wellness of the overall cardiovascular system. A BP that is consistently high means hypertension, which is an important public-health challenge worldwide (5). High BP usually does not cause pains or symptoms, but long-term high BP, which is diagnosed as hypertension, is a major risk factor for coronary artery disease, stroke, heart failure, atrial fibrillation, peripheral vascular disease, vision loss, chronic kidney disease, and dementia (6-9). Hypertension is wide-spread in the US and is the major factor of cardiovascular disease, which was the leading cause of the death in the US in 2014 (10-13). It was reported in a 2002 WHO report that about 62% of strokes and 49% of heart attacks are attributed to hypertension (14).

In order to prevent such critical events by cardiovascular disease, hypertension should be detected and properly managed in an early stage, yet a considerable number of people are ignorant of their BP especially in low resource settings. Thus, they are not labeled as hypertensive, which causes much of the disease burden (15). Although it is crucial to be aware of one's BP status, measurement of BP is mostly performed in a clinical setting with a conventional inflatable cuff-type device that provides only a single or a few BP values, which is not reliable and could even be misleading in representing one's BP status (13). One of reasons for this is the time-varying nature of BP, which shows enormous variability even during a day (16, 17). Pickering et al. pointed out that the correlation between a single measurement of BP and the BP mean during a day is of only 0.5-0.7 (18). In addition, BP can be affected psychologically depending on the situation. When a patient visits a clinical setting, one's BP can be above the normal range and can be falsely diagnosed as hypertension, which is a well-known phenomenon, called the "white coat syndrome" (19). Therefore, the American Heart Association (AHA), American Society of Hypertension (ASH), and Preventive Cardiovascular Nurses Association

(PCNA) recommended the ambulatory BP measurement (ABPM) in 2008 (13) or, in other words, continuous BP monitoring in daily life, which prevents the "white-coat syndrome" effect and enables more frequent BP measurement. Current devices employed for ABPM are usually based on the oscillometric method, which has to be used with an inflating cuff during measurement. However, although many current devices are developed for home and self-use with a simple control, the discomfort of inflating a cuff is a fundamental drawback of cuff-based devices, and the bulky device, which generally consists of an inflating cuff and an air control unit, hinders its frequent use. Particularly, when measurement during sleep is required, a cuff-based device is not a favorable option for users.

If a compact wearable device is designed with a new cuffless modality, which reduces the burden of the inflating cuff, the ultimate goals of continuous, not one-time, BP monitoring, not in a clinical setting but in daily life, will be within reach. As one of the promising cuffless modalities, the pulse transit time (PTT)-based approach has gained popularity and is attracting wide attention.

1.2. PULSE TRANSIT TIME

PTT is the time delay for the BP wave to propagate between two arterial sites (Fig. 1.1). Thus, PTT is in inverse relationship with pulse wave velocity (PWV), which is the velocity of the BP wave propagating along the wall of arterial vessels and is typically faster than the blood flow (20). PWV is known to be closely associated with arterial elastance, which is commonly modeled by Moens–Kortewerg equation assuming an artery as an elastic tube, as follows (21–24):

$$PW\ V = \sqrt{\frac{Eh}{2\rho r}} \quad (1)$$

where E is the arterial elastance, h is thickness of the vessel wall, r is radius of the vessel, and ρ is density of blood. By this model, PTT is inversely related to arterial elastance.

The arterial elastance was empirically modeled by the Hughes equation (25) as follows:

$$E = E_O e^{\alpha P} \quad (2)$$

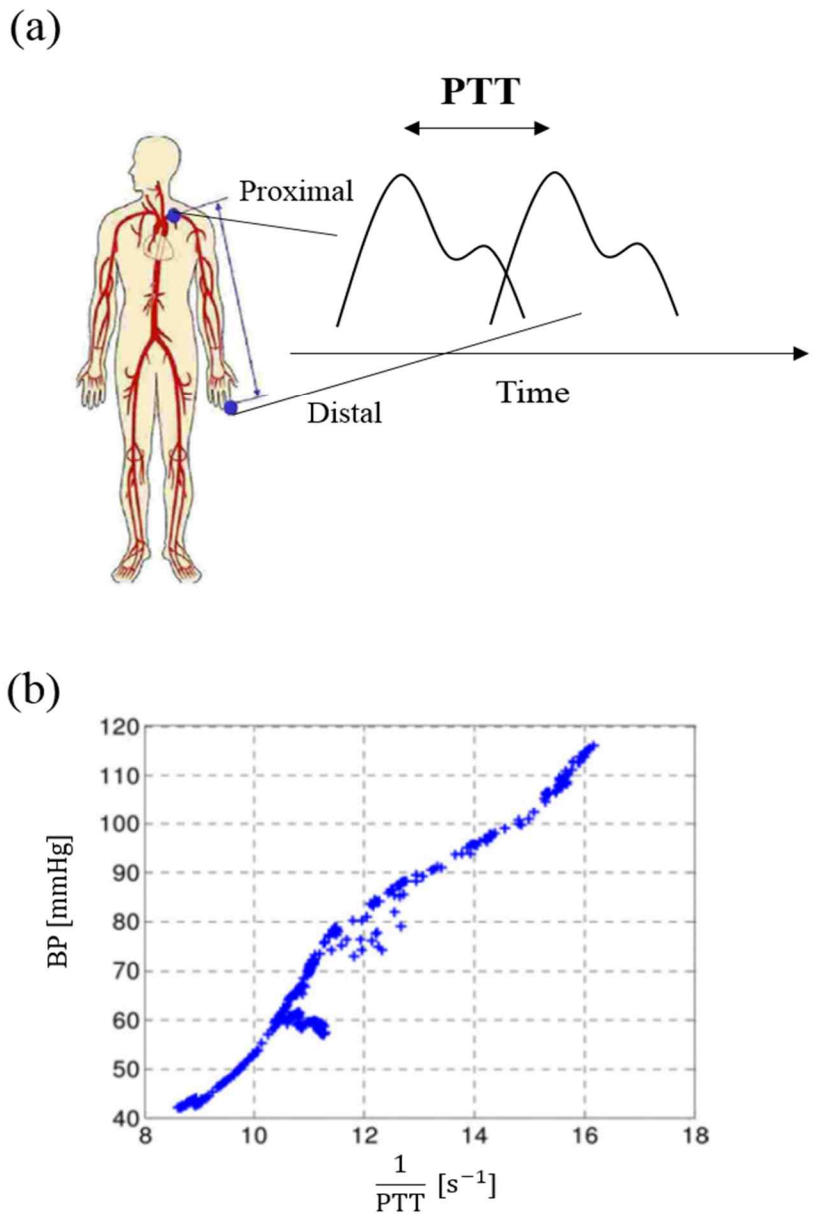

Figure 1.1 Conceptual diagram of PTT–BP relationship. (a) PTT is the time delay for the BP wave to propagate between the proximal arterial site and distal arterial site. (b) PTT is often related to BP.

*The plot in (b) is cited from the review paper by Mukkammala et al. (26)

where E is the artery elastance, E_O is the base elastance, α is a model coefficient, and P is BP. Hughes found out by experimentation that BP is logarithmically related to arterial elastance.

Consequently, combining the two equations above results in the relationship between BP and PWV or PTT, which is written as follows:

$$PW\ V = \sqrt{\frac{E_O e^{\alpha P} h}{\rho 2r}} \tag{3}$$

Squaring both sides and taking the log of each side yields

$$P = \frac{1}{\alpha} \ln PW\ V + \frac{2}{\alpha} \ln \frac{2\rho r}{E_0 h} \tag{4}$$

where the relationship between BP and PWV is explicitly expressed.

Therefore, BP can be theoretically estimated by PWV or PTT based on the equation, and extensive studies have utilized this relationship for continuous and cuffless BP monitoring (see references in the thesis).

Despite a variety of studies attempting to employ the PTT–BP relationship for cuffless BP monitoring, most studies have used the pulse arrival time (PAT) instead owing to its simplicity in measurement (27–32). They measure PAT by employing the R–peak in an electrocardiogram (ECG) as proximal timing reference (timing when the BP pulse begins) and the early rise point of a photoplethysmogram (PPG) as distal timing reference (timing when the BP pulse arrives), and by calculating the time difference between them (Fig. 1.2). The R–peak in an ECG does not represent the beginning of the BP pulse, as a considerable time delay between the R–peak in an ECG and the ejection of blood from the left ventricle (LV) exists (Fig. 1.2). However, it has been widely used to serve as proximal reference as it is thought that the simplicity of using the ECG outweighs the possible issue of including the time delay between the electrical activation of the heart and the mechanical ejection of blood from the LV. In previous studies, this time delay nearly overlapping with the pre–ejection period (PEP), which is defined as the time delay between the Q–peak in the ECG and the aortic valve opening (AO) time and has different mechanisms of responding to a BP change, has been reported to show a

significant adverse effect in using the PTT-BP relationship (26, 33, 34). Therefore, recently, efforts to eliminate the portion of PEP by using different bio-signals other than the ECG have been made (35-38). However, most of the attempted approaches are questionable in terms of practicality as the systems are bulky, consisting of multi modules or requiring intervention of the user, which may deter frequent measurement.

Additionally, even the PEP-excluded PTT has not been providing satisfactory results of BP estimation. While PTT has shown good correlation with the diastolic blood pressure (DBP) or mean blood pressure (MBP), it has showed less satisfying results in terms of relationship with the systolic blood pressure (SBP) (33, 38, 39). PAT has often exhibited a better correlation with SBP compared to PTT (38); therefore, it is often believed that PAT is a better surrogate marker of BP, leading to the claim that PEP should be included (40).

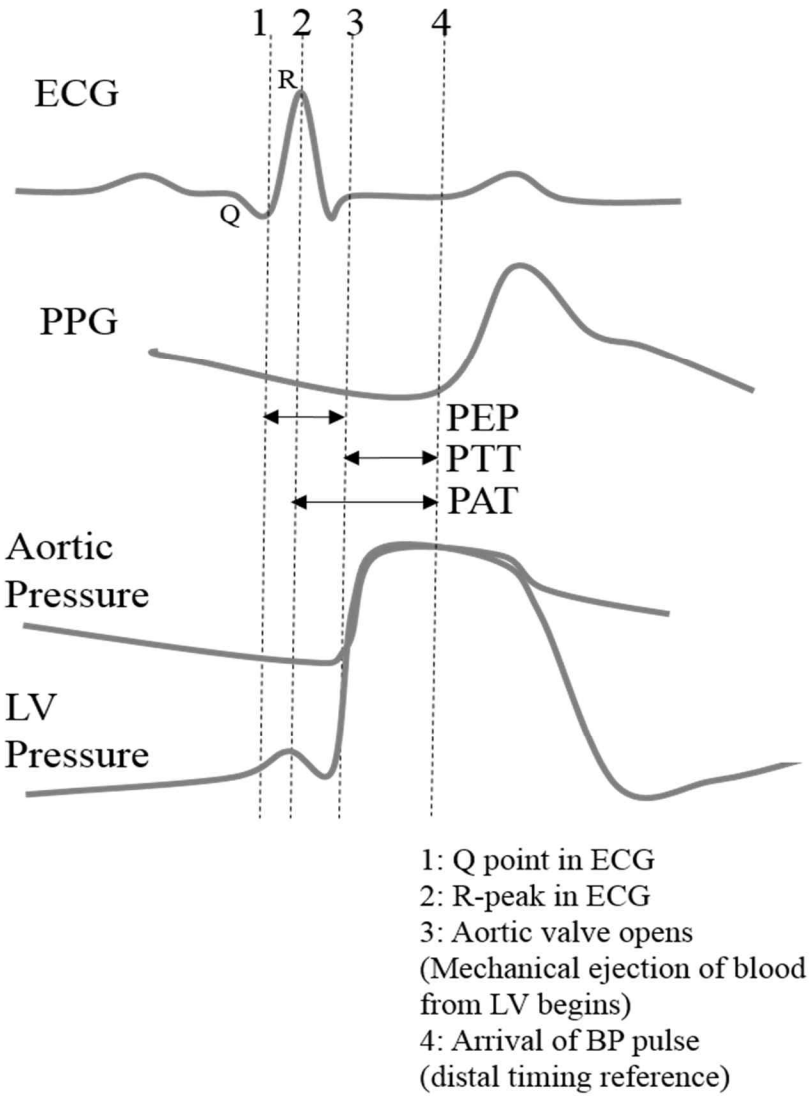

Figure 1.2 Diagram illustrating the relative timing of the ECG and PPG with respect to pressure change in left ventricle (LV) and aorta. Aortic valve opens when LV pressure rises above aortic pressure, and blood begins to be ejected to aorta through the aortic valve. PAT is the time delay between R-peak in ECG (2) and early rise point of PPG (4). PTT is the time delay between beginning of BP pulse (3) and arrival of BP pulse (4). PEP is the time delay between the Q-peak in ECG (1) and the AO time (3).

1.3. THESIS OBJECTIVE

While the modalities proposed so far to serve as proximal timing reference instead of ECG seem to be not adequate for continuous BP monitoring, the seismocardiogram (SCG), the precordial vibration of cardiac movement, has gained wide attention as an alternative signal to provide proximal timing reference. It was shown by previous works that a particular feature point of the SCG waveform coincides with the opening of the aortic valve (41, 42). In addition, SCG can be measured very simply by a tiny accelerometer on the precordial site, compared to the impedance cardiogram (ICG) or ECG, which requires multi electrodes. As the technology in accelerometers advances in terms of size and precision, SCG becomes an appreciable modality to serve as proximal timing reference.

Therefore, the first objective of this thesis is to develop a wearable system realizing cuffless and continuous BP monitoring based on the PTT–BP relationship by measuring SCG and PPG on the chest with a single device. For this objective, we specialize the conventional PPG measurement system to be utilized on the chest and integrate it with the SCG measurement

system. Furthermore, we consider the power consumption of the system and attempt to reduce it, which will facilitate long-term continuous monitoring, which is recommended for diagnosing hypertension (Chapter 2).

The second objective of this thesis is to analyze the current poor relationship between PTT and SBP and improve the performance of the BP estimation. For this objective, we assess the PTT-BP relationship along with PAT in opposite situations and introduce a potential covariate to complement the PTT-BP relationship. Furthermore, we validate the proposed system against the general population and in daily life to demonstrate its potential to real use (Chapter 3).

CHAPTER 2

Development of the Wearable Blood Pressure Monitoring System

2.1. INTRODUCTION

As mentioned in Chapter 1, the modalities to measure the PTT proposed so far are questionable in terms of practicality, not to mention their lack of potential to be utilized in daily life. Most of the previous studies have mainly focused on validating efficacy of PTT in relatively static circumstances or in surgery, which are mostly controlled settings. Efforts to measure PTT in previous research have yielded various bulky system designs. Dual-channel of PPG system attached to both finger and toe sites was proposed and measured the time difference of PAT at each site (35). The use of a combination of ICG and PPG was often proposed to measure PTT (36, 37). A combination of ballistocardiogram (BCG) and PPG was also studied (38). However, although those systems could provide the means of measuring PTT, both BCG and ICG are difficult to measure in a wearable device to enable daily monitoring.

Recently, SCG, precordial vibration of the cardiac movement, has attracted wide interest as a signal that provides rich information with regard to cardiac motions (41, 43-45). It was shown by previous works that a particular feature point of the

SCG waveform coincides with the opening of the aortic valve simultaneously observed by an echocardiogram (41, 42). However, use of the SCG is, owing to the signal source, limited in terms of measurement sites. SCG is usually measured on the vicinity of the sternum, which hinders its combination with PPG, serving distal timing reference, as it is difficult to acquire a high-fidelity PPG waveform on the chest surface, which lacks of blood perfusion compared to other locations, such as the finger-tip, toe, and ear.

In this chapter, we aim to develop a single wearable device to measure PTT by measuring PPG and SCG on the chest. For this purpose, we address the difficulty of measuring PPG on the chest by specializing the PPG measurement system and lower the power consumption of PPG and the whole system to realize continuous and long-term BP monitoring.

In addition, the repeatability of BP-related parameters derived by the developed device is tested to verify the possible variability when wearing the developed device repetitively. Lastly, we examine whether the derived PTT using SCG and PPG

truly excludes any portion of the PEP and contains the artery information.

2.2. SYSTEM OVERVIEW

The core design of the proposed system aims to enable the measurement of PPG and SCG on the chest with a single compact and light device. Figure 2.1 shows the overall system block diagram, consisting of bio-signal sensors, pre-amplification analog circuits, digital circuits, power management unit, communication unit, and external data acquisition units. Three types of sensors were employed. For PPG and SCG instrumentation, three pairs of photodiodes and light emitting diode (LED), and one analog accelerometer were employed, respectively. In addition, ECG electrodes were used for an auxiliary purpose: to assist signal processing for its robustness against noise, and to compare the reference PEP and the portion of PEP obtained by the combination of ECG and SCG, which will be explained, respectively, in the following “Signal processing” and “Experimental setup” sections.

An analog circuit was minimally designed. Only a simple and basic analog circuit, such as a trans-impedance inverter (TIA), a first-order low pass filter, was used. However, our design employs a high resolution analog digital converter (ADC, ADS1298, TI, US) to complement resolution problems, as the phase distortion by the analog filter is a crucial issue when calculating the time difference of signals. Most of the filtering and amplification was conducted in the software, as explained in the "Signal processing" section. It is noted that a feedback loop was constructed for PPG instrumentation consisting of the ADC, digital-to-analog converter (DAC), and micro control unit (MCU) to increase the PPG signal-to-noise ratio (SNR), which will be explained in detail in the following section.

The system power was delivered by a lithium polymer battery (30 mm * 25 mm * 4 mm, 280 mAh) designed to be recharged with a micro USB cable, as it is done in a mobile phone, for continuous monitoring in daily life.

The acquired and digitized signal data were transferred via a Bluetooth module (BoT-CLE310, Chipsen, South Korea) to an external data acquisition system, such as a mobile application and

PC software platform, which were also developed for convenient and practical use of the system. This is explained in detail in the “Software development" section.

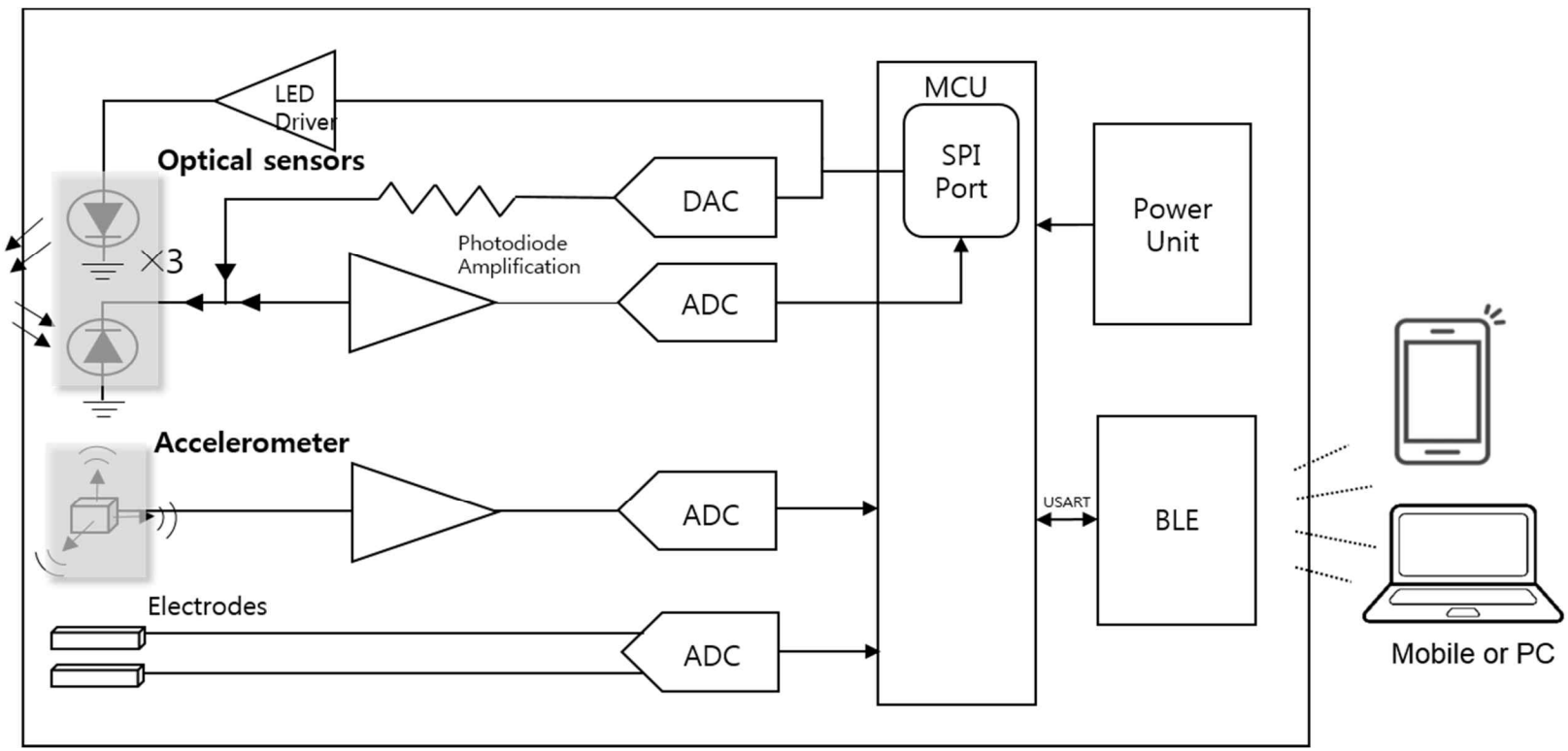

Figure 2.1 System block diagram. The system consists of bio-signal sensors, pre-amplification analog circuits, digital circuits, power management unit, communication unit, and external data acquisition units

2.3. BIO-SIGNAL INSTRUMENTATION

In order to measure PPG on the chest, three pairs of optical sensors, each consisting of one 850 nm wavelength infrared LED (SFH4059, OSRAM, Germany) and two photodiodes (VBP104S, Vishay, US), were used to enhance the SNR of the PPG. The three optical sensor pairs were placed apart from each other to widen the sensing area, as the blood perfusion beneath the skin of the chest is not abundant for PPG measurement compared to other areas, such as the finger, earlobe, and toe that are traditionally used as PPG measurement sites. Each output current from the three optical channels was converted to voltage using a trans-impedance amplifier (TIA) circuit.

In order to boost the SNR of PPG, a DC offset subtraction feedback loop was employed. This loop monitored the DC level of PPG by MCU, which is directly proportional to the amount of light emitted from the LED. Depending on the current DC level, the MCU decided the corresponding output of DAC, and thereby controlled the offset current using a feedback resistor (Fig. 2.2a), which prevents the circuit from the saturation frequently occurred by the high intensity of light. Thus, this enabled to use

high intensity of light without the worry of saturation, which results in a high SNR of the PPG.

For SCG, the anteroposterior axis output of a low-power analog accelerometer (ADXL327, Analog Devices, US) was used. The accelerometer was with a full-scale range of $\pm 2g$, and this small full-scale range may be appropriate for sensing a low level of vibration, such as that of the SCG. An internal low-pass filter with cutoff frequency of 50 Hz was used to suppress aliasing in the ADC process.

For simple ECG measurement, a widely used two electrode-configuration was employed with common-mode biased voltage. The electrode metals were a copper base coated with platinum to increase bio-compatibility, forming a single lead with 5 cm distance across the chest.

In order to prevent the phase shift of signals, which may affect the inter-waveform time measurements, all signals were digitized using the aforementioned high resolution 24-bit analog-to-digital converter (ADS1298, TI, US) without any analog filter, with the exception of the internal low pass filter of the SCG channel.

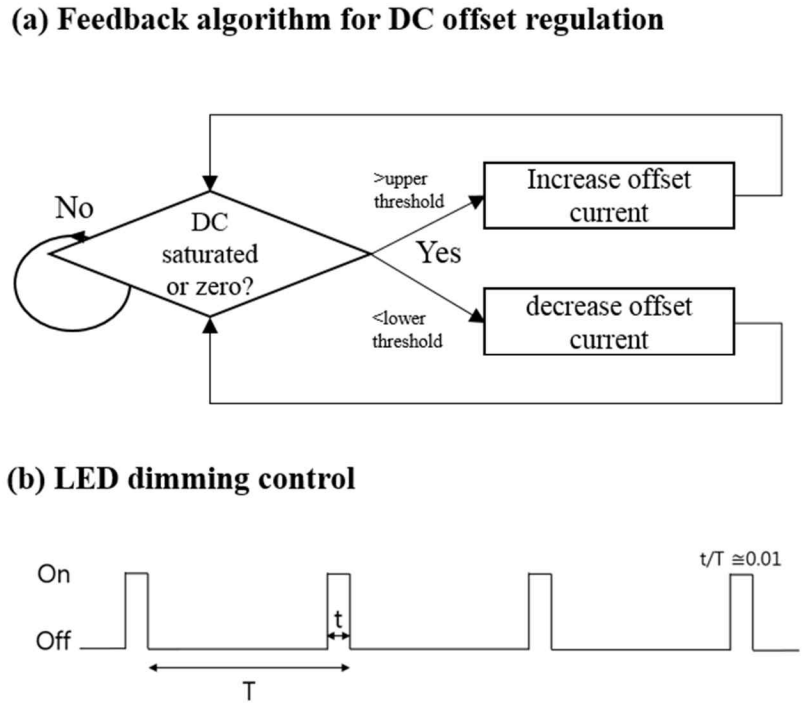

Figure 2.2 Specialized technique applied to the system. (a) Feedback algorithm to maintain proper DC offset level. Depending on whether DC offset is saturated or zero, the offset current is regulated. (b) LED dimming control scheme to reduce LED power. LED turned on every a hundredth of a period (t/T~**0.01**).

2.4. POWER MANAGEMENT

The hardware was designed to reduce power consumption in order to enable continuous monitoring in a long-term period. We used three LEDs consuming up to 180 mA (60 mA each) in total during normal operation to acquire PPG in the chest. However, we employed the strategy that controls the dimming frequency and timing of the LEDs. As Fig. 2.2b shows, during one period of ADC sampling, the LED turned on every a hundredth of a period (T) , which lowered the current consumption of the LED down to 1 % of that in normal operation and enabled to cut down much of the power consumption of the whole system. Additionally, using a Bluetooth low energy (BLE) module and MCU (ATMEGA168, Atmel, US), the whole system consumes less than 10 mA during monitoring, enabling more than one day of continuous monitoring with a 280 mAh small-sized lithium polymer battery.

2.5. PRINTED CIRCUIT BOARD AND CASE DESIGN

Not only the circuit system but also the design of the printed circuit board (PCB) and the case were carefully considered to improve contact with the curved chest.

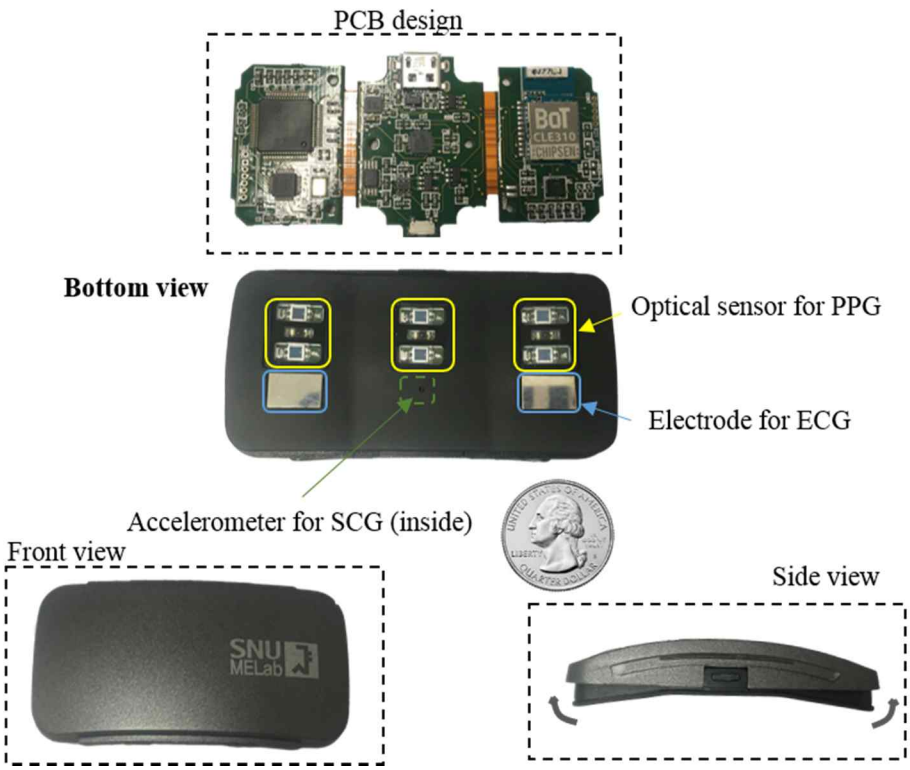

Figure 2.3 Printed circuit board and case design

All analog and digital circuits were implemented on a customized PCB comprising three rigid pieces connected by flexible bridges to flexibly conform to the curvature of the torso (Fig. 2.3).

The flexible printed circuit board was encased in a curved hard-case, which is also capable of flexion depending on the curvature of the torso (Fig. 2.3). The developed device measured 40 mm in length, 76 mm in width, 18 mm in thickness, and weighed 27.5 g, including the hard case. (Fig. 2.3).

2.6. SOFTWARE DESIGN

Two types of data acquisition platforms were developed. First, mainly for the purpose of validation in in-lab condition, where a PC is easily equipped, a PC-based graphical user interface (GUI) software was developed (MATLAB 2018a; The MathWorks, MA, USA). This collects data from the developed device via a serial port and displays the raw waveforms of three signals (PPG, SCG, and ECG) and the processed signal in one heart beat period along with the reference BP, which is recorded simultaneously for validation in the BP estimation stage. The signals and reference BP are easily saved by pushing the designated button, and the time lapse is also shown in the front to track the recording time (Fig. 2.4a)

The second platform is the mobile application for the purpose of daily monitoring. The mobile application is based on Android OS and is not supported for the IOS. It automatically pairs with the developed device and collects the data in a daily life. It displays the raw signals, processed parameters such as PAT, PTT, and HR, and the final estimated BP, depending on the user's choice (Fig. 2.4b). By setting the period of trend view longer, users can

track one's BP during a long time, and thus, evaluate one's BP changes in real practice.

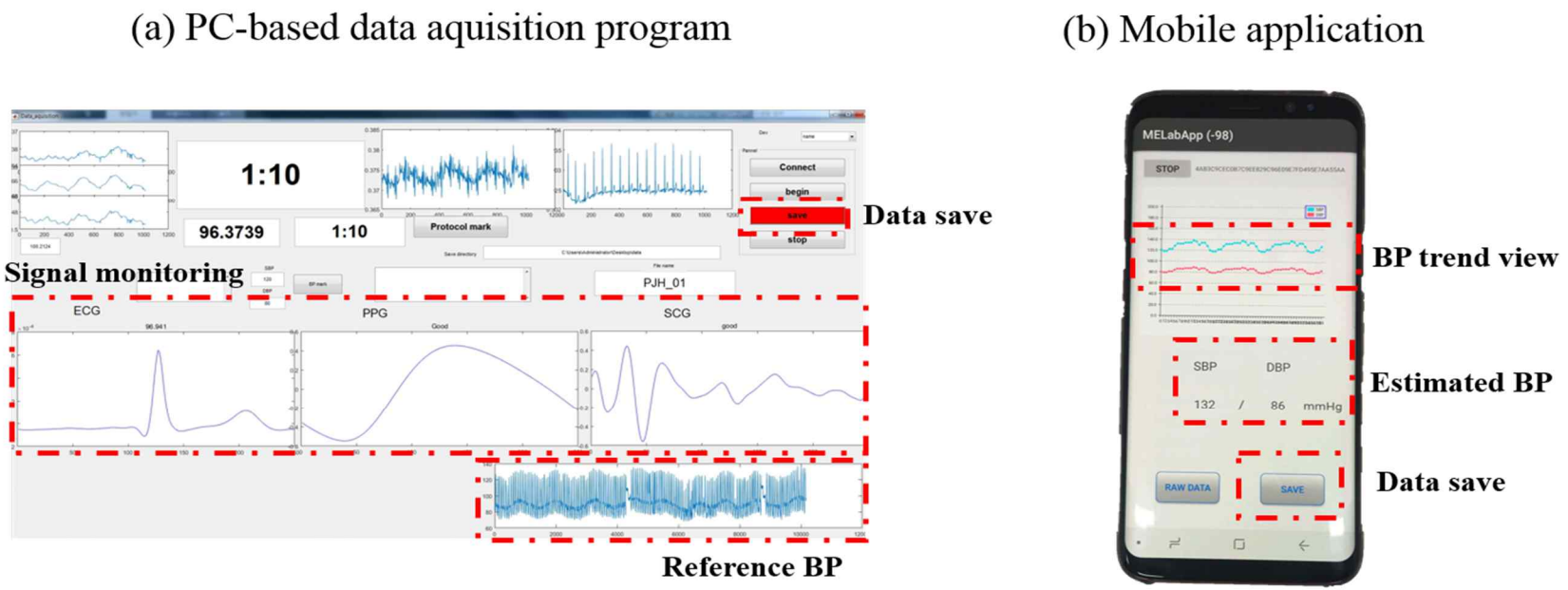

Figure 2.4 Data acquisition program. (a) A PC-based graphical user interface data acquisition program was developed, which was designed to show the processed signal in one heart beat period along with the reference BP. (b) Mobile application based on Android OS was designed to auto-connect with the developed device, save received data, and show processed signals, parameters, and estimated BP.

2.7. SIGNAL PROCESSING

The acquired raw signals were processed using MATLAB to remove noise from the motion artifact, baseline wandering, and respiratory signal. The SCG and ECG signal was band-pass filtered with cutoff frequencies at 0.3 Hz and 50 Hz. The raw PPG signals from three optical channels were low-pass filtered with a cutoff frequency of 10 Hz considering the frequency characteristic of PPG, and high-pass filtered with a cutoff frequency of 0.3 Hz. Digital filters without phase shift were used to prevent signal shifting during filtering.

Afterwards, we employed the ensemble averaging method to extract the averaged signal in one cardiac cycle. In 10 s of signals, the ECG R-peaks were identified for the ensemble standard. PPG and SCG signals between two consecutive R-peaks were segmented and all segments of PPG and SCG between two consecutive R-peaks were averaged, which results in one waveform for PPG and SCG in a single cardiac beat in 10 s.

Regarding PPG, as three channels of PPG were used, we obtained three PPG waveforms. A single PPG waveform was chosen based

on the developed criteria. Figure 2.5.1 shows the various conditions the PPG waveform should meet. These conditions were imposed considering the typical PPG waveform and morphology variability. Based on the number of conditions that a waveform meets, an optimal channel was decided. If no waveform could meet more than 5 conditions, no channel was selected.

After one PPG waveform and one SCG waveform were obtained, the characteristic points were detected. In the SCG waveform, the maximum peak, named AO according to the designation of early works on SCG (44, 45), was detected, the timing of the maximum peak was calculated, and the maximum amplitude of the SCG waveform (maximum downward peak prior to the AO point – maximum peak) was regarded as the SCG amplitude (SA). In the PPG waveform, the intersecting tangent (IT) point (46) (which is the intersecting point between the tangent to the PPG max slope and the tangent to the diastolic minimum) was detected. Using the AO point and PPG IT point, SCG–PEP and PAT were calculated, respectively, and the time difference between those was regarded as SCG–PTT (Fig. 2.6)

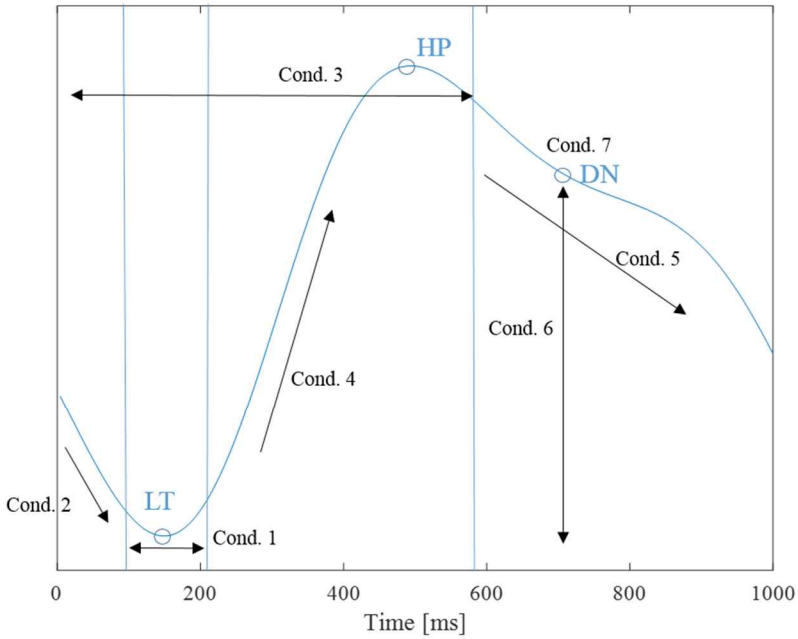

Condition 1.
Lowest trough (LT) is located in proper range.

Condition 2.
Between first point and LT, waveform should monotonously decrease..

Condition 3.
Higest peak (HP) is located in proper range.

Condition 4.
Between LT and HP, waveform should monotonously increase.

Condition 5 .
Between HP and end point, waveform should decrease with proper inflexion point.

Condition 6 .
Between HP and end point, dicrotic notch (DN) should not be lower than LT.

Condition 7.
DN is captured.

Figure 2.5 Criteria for assessing quality of PPG waveform. One PPG channel was decided by the developed criteria based on morphological analysis of PPG waveform. At least 5 conditions should be met.

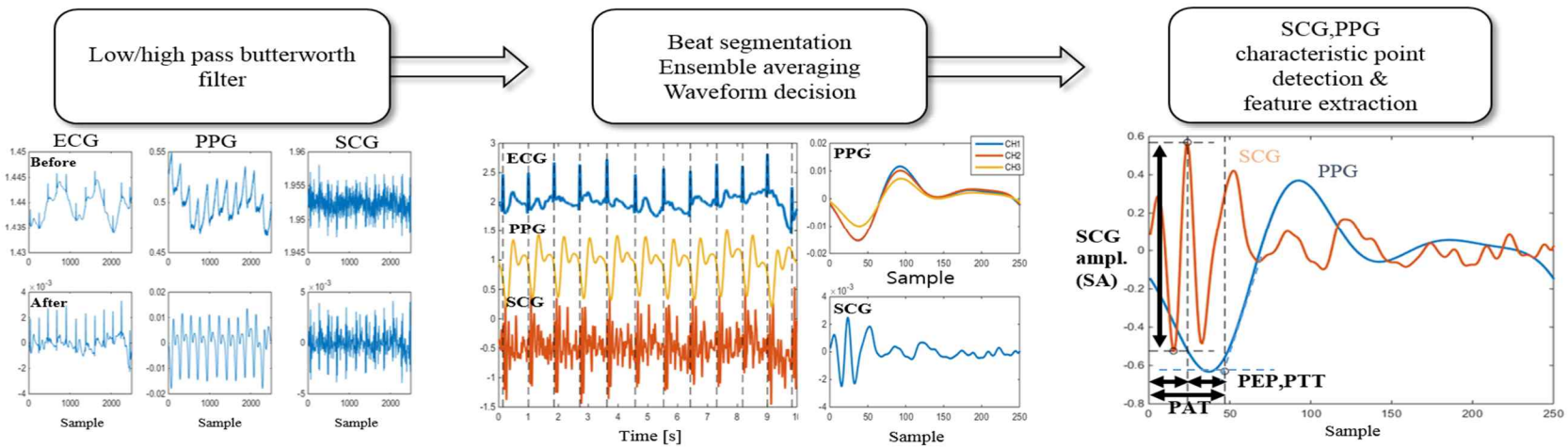

Figure 2.6 Flow chart of signal processing. First, acquired signals were low- and high-band pass filtered with different cutoff frequency bands depending on the signal (0.3–10 Hz for PPG, 0.3–50 Hz for ECG and SCG). Then, heart beat was segmented by R-peak detection and, using the ensemble averaging technique, PPG and SCG waveforms from each heart beat period were averaged, resulting in one waveform of PPG and SCG. A single PPG waveform was chosen based on the developed criteria. Afterwards, in SCG waveform, maximum peak and maximum downward peak prior to AO point were detected and SA was calculated. In PPG waveform, intersecting tangent (IT) point was detected and PTT was calculated between AO point and PPG IT point.

2.8. EXPERIMENTAL SETUP

2.8.1 Repeatability test

In order to assess the repeatability of the calculated BP-related parameters, 10 subjects wore the developed chest-worn device twice, with 5 min of interval. At the first trial, a subject wore the developed device under the guidance of the researcher involved in this study. At the second trial, the subject wore it without any guidance, as similar as possible to the first trial. The guideline just told the subjects that the device should be located approximately 5 cm below the left nipple. An elastic strap connected with the device supporting frame, which was customized along with the device, was used to hold it. By the benefit of the elastic strap, the length of the strap surrounding the chest could be customized for each subject, with the result that the contact of the device with the chest remained uniform for repetitive wears and measurements. For each trial, subjects were seated and asked to remain still for 1 min. Between trials, subjects were asked to refrain from excessive movements or activities in order to hold the same hemodynamic states, including BP and HR, for each measurement, so that only the effect of the repeated measurement could be observed. The repeatability of the parameters was evaluated by intra-class correlation (ICC), with significance level < 0.5. An ICC > 0.8 generally shows that the repeatability of measurements is very good.

2.8.2 Verification of SCG-based PEP

The experiment to verify the measured SCG-based PEP in short-term hemodynamic changes was performed.

In total, 17 males (27.9 ± 1.7 year old) subjects, without any previous history of cardiovascular conditions, were recruited. Informed consent was obtained from all individual participants included in the study. The developed device was attached to the skin over the 6^{th} left costal cartilage of each subject. For reference, electrodes for ICG (Cardioscreen 1000, Medis, Germany) were attached to the neck and torso to detect the true aortic opening time (Fig. 2.7). After device placement, all the subjects stood still for 20 s for a rest phase recording. Then, to induce hemodynamic changes, they were instructed to form a squat posture without upward movement for 100 s, followed by a recovery phase in an upright position for 120 s.

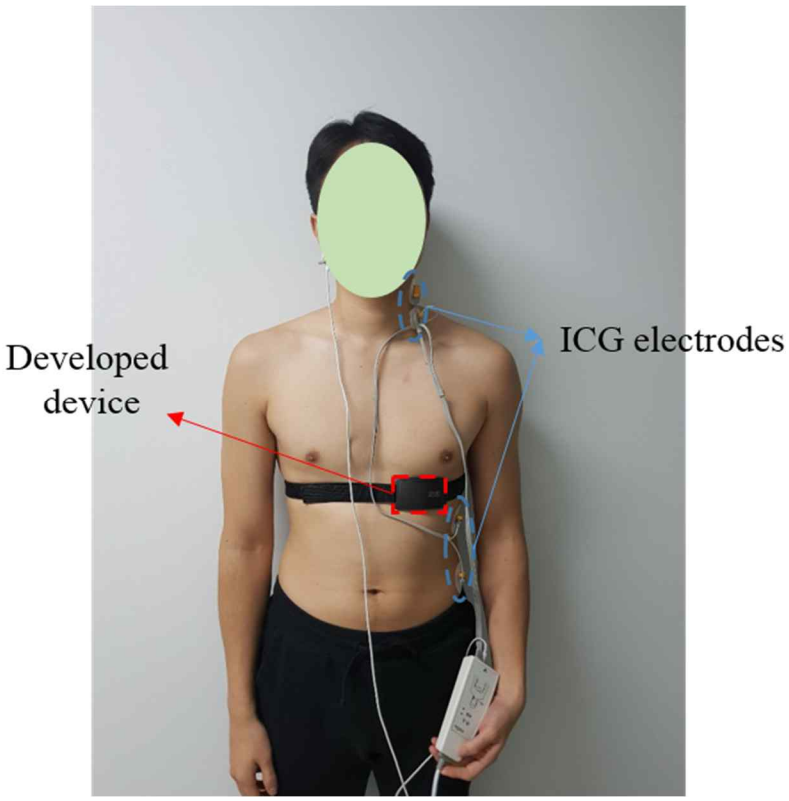

Figure 2.7 Setup for PEP comparative study

The reference PEP, which is defined as time difference between the Q point in ECG and B-point of ICG, was provided by the ICG device

In order to directly compare SCG-PEP, which is defined in this study as the time difference between the R-peak of ECG and AO point in SCG, the Q-R interval time in ECG was subtracted from ICG-PEP (Fig. 2.8).

We compared the group averaged value of ICG-PEP and SCG-PEP from all subjects in three periods during the hemodynamic change: 1) rest value of ICG-PEP and SCG-PEP averaged over 20 s in the early beginning of the rest phase, 2) extreme value of ICG-PEP and SCG-PEP averaged over 20 s around the time when each PEP value dropped to minimum in the exercise phase, and 3) recovered value of ICG-PEP and SCG-PEP averaged over the last 20 s of the recovery phase. A paired t-test was used to analyze the statistical difference between the values of ICG-PEP and SCG-PEP in the three periods.

In addition, the group average of individual correlation coefficients between values of ICG-PEP and SCG-PEP during whole period of hemodynamic change was computed.

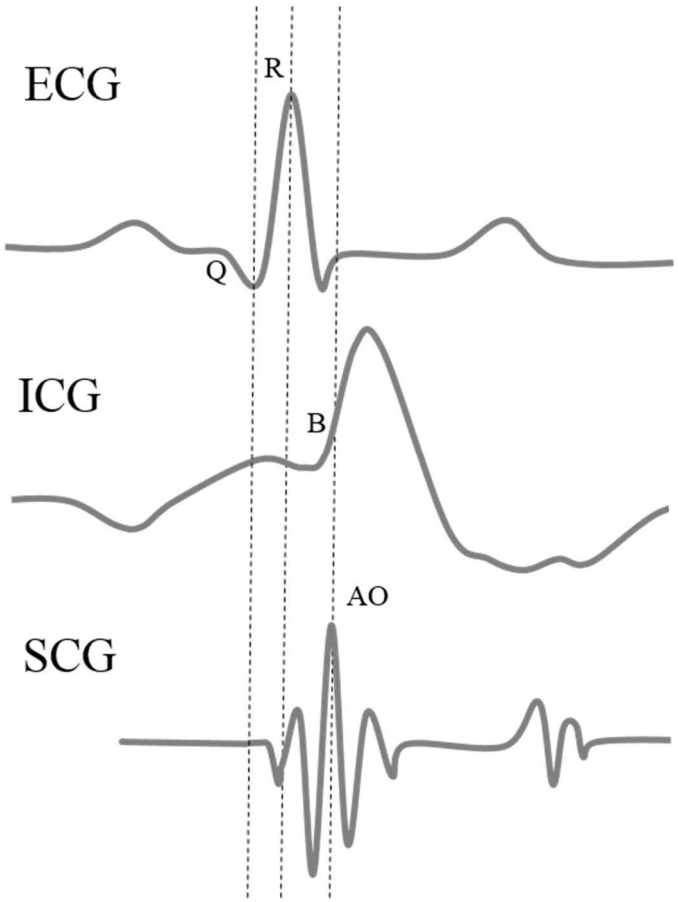

Figure 2.8 Typical waveforms of ECG, ICG, and SCG. PEP is defined as time difference between Q point in ECG and B point (zero crossing point) in ICG. In this study, in order to directly compare SCG-PEP, which is defined as the time difference between R-peak of ECG and AO point in SCG, Q-R interval in ECG was subtracted from ICG-PEP.

2.9. RESULTS & DISCUSSION

2.9.1 Repeatability test

ICC scores of the repetitive measurements were 0.87, 0.83, 0.78, and 0.95 for PAT, PTT, PEP, and SA, respectively. P values for each ICC result were <0.001, <0.001, <0.05, and <0.001, exhibiting a significant level. All parameters showed very good repeatability between measurements (Fig. 2.9). Particularly, SA showed excellent agreement between two measurements, even though, in general, the bio-signal amplitude can be easily altered by repetitive contacts.

The possible explanation for this robust consistency might be that the cardiac vibration can be transferred relatively and consistently to a large area of the chest skin via the chest wall surrounding the heart, which allows the device to capture a consistent SCG waveform even in different locations by repetitive wears. In addition, the dimension of the developed device enables it to cover a large area of the chest skin, which allows to measure SCG consistently, without a strict restriction of sensor location.

Repeatability of the parameters can be of importance for the purpose of daily life monitoring. As a user often wears and takes off the device during monitoring in daily life, if the parameters are not consistent between repetitive wears, the reliability of a BP estimation based on the parameters may not be assured. It is viable to require the user not to take off the device during monitoring, but this may cause discomfort to the user during the monitoring period, which could deter its long-term use.

Figure 2.9 shows that the parameter baseline values are variable between individual subjects, especially for SA. As the force of cardiac contraction, how the vibration transfers to the measurement site via the chest wall, and the tightness of contact of the device to the chest vary by subject, the baseline SA can be different for the subjects. Other time parameters also showed individual differences, to a lesser degree. However, the baseline differences between subjects would not matter if individual calibration, requiring either single or multiple measurements, is carried out before use.

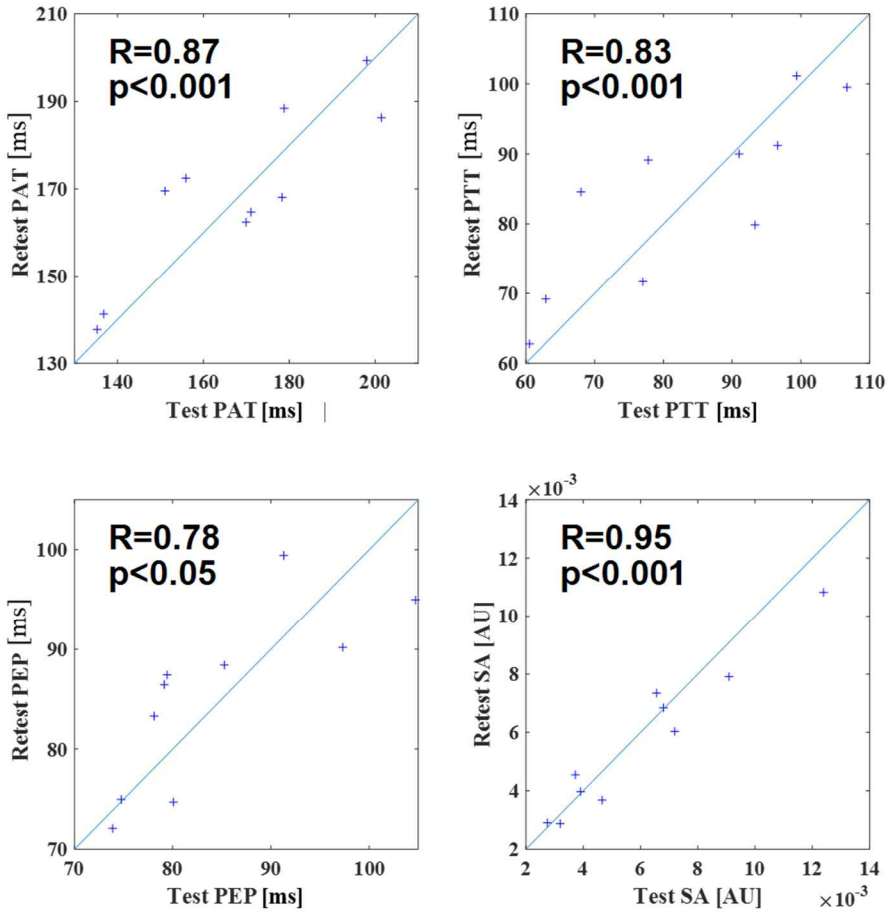

Figure 2.9 Test–retest result of parameters. The subjects wore the device twice with interval of 5 min. Parameters were extracted for two trials and compared, resulting in good repeatability.

2.9.2 Verification of SCG-based PEP

The rest values of ICG-PEP and SCG-PEP were 76.51 ± 13.14 ms and 74.09 ± 13.77 ms, respectively, while when the hemodynamic change was maximal, the values of ICG-PEP and SCG-PEP were 50.79 ± 9.77 ms and 57.50 ± 10.84 ms, respectively. In recovery, the values of ICG-PEP and SCG-PEP were 68.98 ± 14.70 ms and 72.16 ± 13.43 ms, respectively. While two PEPs showed nearly identical values in the rest period, the difference between two PEPs was relatively larger when they were minimal. After the hemodynamic change was considered recovered, the difference between two PEPs was not of the same degree compared to the difference in the rest condition. However, in all periods, any statistical difference was not found. Figure 2.10 shows a comparison between the group trend of ICG-PEP and SCG-PEP during the hemodynamic change, which verifies a nearly similar trend of change between two PEPs and negligible difference given the standard deviation. In addition, the group correlation coefficient was of 0.79 ± 0.14, which suggests a tight correlation between two PEPs even under excessive hemodynamic change.

Previous studies have verified that the SCG-based PEP is equivalent to the standard ICG-measured PEP in the resting condition (47) and the PEP measured using an echocardiogram (42). However, it was still unclear whether this relationship is held during large hemodynamic fluctuations. It was found, even in the period when hemodynamic conditions were greatly altered, that the SCG-PEP value remained close to ICG-PEP. Further, the high correlation values between SCG-PEP and ICG-PEP provide evidence that this relationship

remains unchanged throughout the induced cardiovascular change (SCG−PEP will be called PEP hereafter). This, in turn, suggests that SCG−PTT, defined as the time difference between the AO point in SCG and PPG IT, can truly exclude the PEP component in a change of the hemodynamic system (SCG PTT will be called PTT hereafter).

Table 2.1 Comparison between ICG−PEP and SCG−PEP values. Group average of ICG−PEP, SCG−PEP values in the rest phase, intervention period, and recovery phase for all subjects were compared. HR at each phase was calculated to assess hemodynamic change during the protocol. A null hypothesis was that difference between two groups does not exist, and p value indicates that null hypothesis cannot be rejected for all phases. Group average of individual correlation coefficients between ICG−PEP and SCG−PEP was also calculated.

	Rest	Intervention period	Recovery	Correlation
HR	89.22±11.44	102.06±12.17	89.06±13.08	-
ICG-PEP	76.51±13.14	50.79±9.77	68.98±14.70	0.79±0.14
SCG-PEP	74.09±13.77	57.50±10.84	72.16±13.43	
p value	0.61	0.12	0.52	-

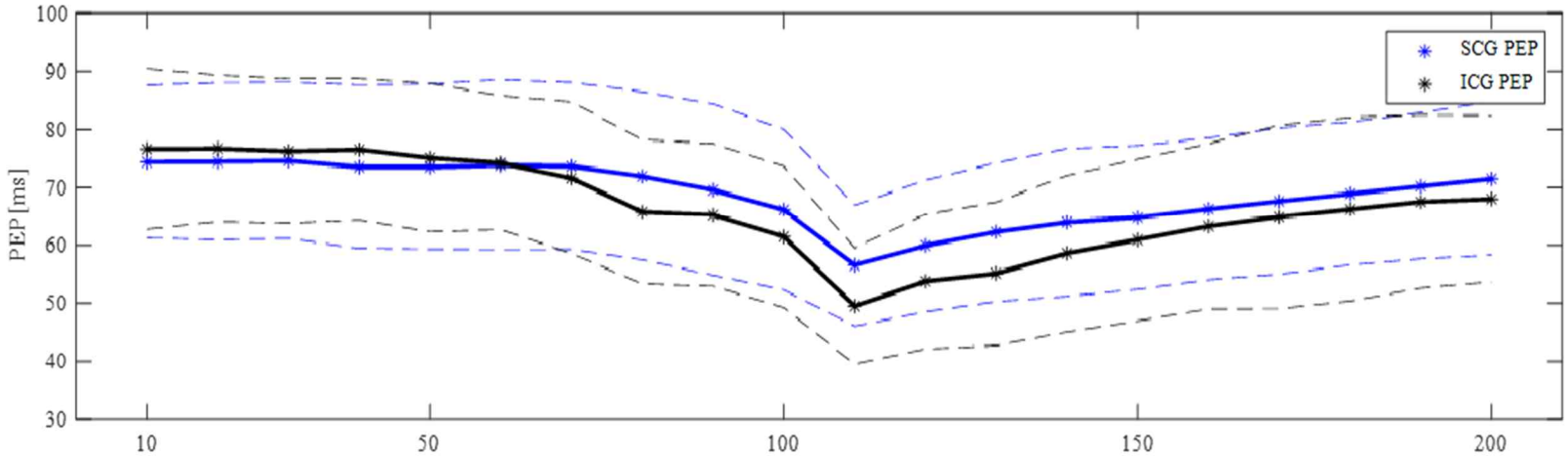

Figure 2.10 Comparison between the group trend of ICG−PEP and SCG−PEP change during hemodynamic change. For visual comparison, ICG−PEP and SCG−PEP were averaged over every 10 s, and in total 20 pairs were acquired for each subject. For every pair, mean values of SCG−PEP and ICG−PEP from all subjects were computed, respectively. Dash line represents mean ± standard deviation for each PEP.

CHAPTER 3

Enhancement of PTT-based BP estimation

3.1. INTRODUCTION

Although PTT is the most potential surrogate marker of BP as it is firmly based on the PTT–BP relationship, it has not been providing promising results, especially for SBP estimation. In previous studies, Zhang et al. directly compared PAT and PTT, and concluded that PTT was not as effective in SBP estimation as in DBP or MBP (33). Nurnberger et al. found that PTT only correlated with DBP (39). Kim et al. studied the efficacy of BCG–based PTT measurement and compared it with conventional PAT. They found that BCG–based PTT was correlated well with DBP and MBP, but PAT outperformed PTT in SBP (38). Recently, it was suggested that the principle of PWV is theoretically more applicable to DBP or MBP (26, 39, 50) as arterial elastance is a function of blood pressure averaged over a long period of time, which can be approximated to MBP or DBP. Furthermore, it is evident that PTT, as a single variable, may not be able to track two different BPs unless the two targeted values are tightly correlated, showing the same movements in both cases. Although two BPs are highly correlated in general, it has been reported

that the correlation between two BPs decreases in certain cases and is not always excellent (48, 49).

Thus, attempts have been made to independently estimate the difference between SBP and DBP, the pulse pressure (PP), which causes uncorrelated movements of BP and thereby may degrade the performance of the PTT-based approach, and to summate the estimated DBP and PP to derive the estimated SBP (31, 32). However, those studies were based on PAT, not on PEP-excluded PTT.

As PP depends on cardiac ejection, arterial stiffness, and timing of wave reflections (51, 52), the PTT related with arterial stiffness may be insufficient to account for changes in PP, whereas the arterial stiffness is the major determinant of DBP by the vessel wall properties. In addition, the rise in PP is often more attributable to an increase in cardiac ejection (52). Hence, an indicator of cardiac ejection may help estimate PP along with PTT, and thus, complement the SBP estimation previously performed with only PTT.

Recently, SCG has attracted interest for its rich information on cardiac movement, and features derived from SCG have been

validated for estimating the cardiac ejection (41, 44). Thus, SCG could be utilized not only to serve as proximal timing reference but also as an indicator of PP.

Therefore, in this chapter, we aim to propose a new model to complement the SBP estimation by incorporating one of the SCG parameters, the early peak amplitude of SCG (SA), as a potential indicator of PP considering the association between SA and cardiac ejection (44, 53–56). For this aim, this chapter consists of three stages of study: 1) we validate the proposed model against a conventional univariate model using PTT or PAT in two contrary situations where PP and DBP dominantly change, respectively. Furthermore, beyond the individualized model, which requires individual fitting of the model (demanding a BP change for the individual to fit the model coefficients, and thus, it lacks practical aspects). 2) We generalize the model, which only requires single measurements of BPs and BP-related parameters, and evaluate its performance according to the recent released IEEE standard. Finally, 3) we validate the performance of the model in daily life, which is a totally uncontrolled setting, so that the robustness of the model can be assessed in arbitrary circumstances.

3.2. METHOD

3.2.1 Principle of BP estimation

In deriving eq. 4 in Chapter 1, BP is originated from Hughes equation (25), in which, according to his research, BP indicates the mean arterial blood pressure (MBP). Therefore, many research groups consider PTT as a marker of MBP (37, 50, 57, 58). Other researchers believe that PTT should best correspond to DBP because PWV initiates in a diastole state and the level of the waveform feet is DBP (26, 34, 38). The author of the present thesis will follow here the latter group, and thus, estimate DBP using PTT. However, as MBP is more closely related to DBP than SBP and it is rare that DBP and MBP move in different directions, it is thought that the two approaches would not yield great differences in terms of error.

Rewriting eq. 4, with substitution of BP as DBP, results in the following equation:

$$DBP = \frac{1}{\alpha}\ln PW\ V + \frac{2}{\alpha}\ln\frac{2\rho r}{E_0 h} \qquad (5)$$

If PWV is substituted with L/PTT, where L is the certain pulse travel distance,

$$DBP = -\frac{1}{\alpha}\ln PTT + \frac{2}{\alpha}\ln\frac{2\rho r}{E_0 h} + \frac{1}{\alpha}\ln L \quad (6)$$

On the other hand, PP was approximated by linear modeling using SA, based on the potential of SA to reflect stroke volume (SV).

$$PP = p_1 SA + p_2 \quad (7)$$

Where p_1 and p_2 are linear coefficients relating SA with PP.

Consequently, SBP can be derived by summating DBP and PP, estimated by PTT and SA, respectively, as follows:

$$SBP = -\frac{1}{\alpha}\ln PTT + p_1 SA + \frac{2}{\alpha}\ln\frac{2\rho r}{E_0 h} + \frac{1}{\alpha}\ln L + p_2 \quad (8)$$

Further, SBP and DBP can be rewritten in a simplified form as follows:

$$SBP = a \ln PTT + bSA + c \quad (9)$$

$$DBP = a' \ln PTT + b' \quad (10)$$

where a, b, c, a', and b' are treated as subject-specific parameters.

3.2.2 Subjects

Under the Institutional Review Board approval obtained from the College of Medicine in the Seoul National University and Hospital (IRB No. H-1701-111-826), a total of 30 male subjects (31.47 ± 7.23 years of age), without any previous history of cardiovascular conditions, were recruited. Informed consent was obtained from all individual participants included in the study. For the first stage of the study, where the proposed model is compared with the conventional models in two different interventions, 10 male subjects (29.70 ± 5.46 years of age) were first recruited. One subject was excluded owing to signal distortion by excessive motion of the artifact during the protocol.

The volunteers were young and healthy, and their BP range was in a normotensive range.

For the second stage of the study, 20 subjects, whose demography was relatively more diverse than the subject pool in the first study, were recruited afterwards. The detailed demography is presented in Table 3.4.

For the last stage of the study, to monitor BP in daily life, nine subjects, who have already taken part in the previous stages, volunteered.

As the subjects were enrolled in different periods depending on the purpose of the study, the number of participants and demography of the subject pool was different according to the study protocol, and this is explained in detail in the "Study protocol" section.

3.2.3 Study protocol

We designed the study protocol for the purpose of this chapter. First, in order to validate the efficacy of the model in the contrary

interventions, the subjects were asked to wear the developed device around the chest as described in Chapter 2 and the finger-cuff type reference BP measurement device (Finometer, Finapres Medical Systems, Netherlands), which is based on a volume-clamp method. We acquired the bio-signal data from the developed device and the reference BP while inducing BP changes in two ways (Fig. 3.1 and 3.2). The two types of intervention employed were cycling and head down/up (HDU) tilt, each of which induces dominant changes in PP and DBP, respectively. Cycling is one of the widely used interventions to perturb BP (40, 62-65), especially because it can greatly increase BP with ease. During cycling, the activated sympathetic nerve greatly increases HR and SV, and thus, cardiac output (CO), while total peripheral resistance (TPR) is decreased owing to vascular dilation in the active muscle (66), which results in a relatively small increase in DBP and great increase in SBP. Therefore, we regarded the cycling test as a PP dominant BP change protocol.

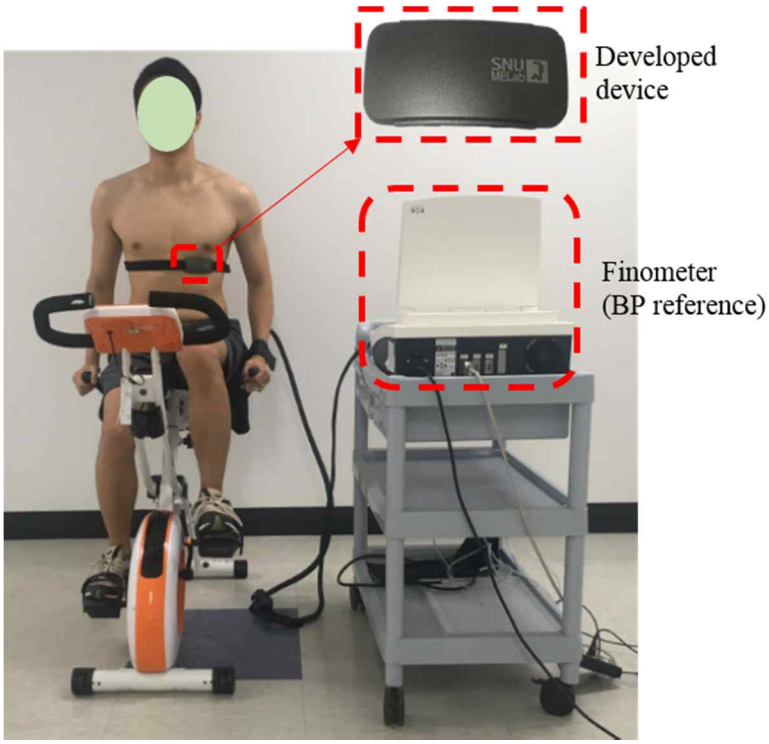

Figure 3.1 Subject cycling with the developed device and reference BP

For the second type of intervention, a HDU change was performed. Orthostatic stress occurs when a subject stands up quickly, which causes the reduction of venous return due to pooling of the blood volume in the lower body by the gravitational force (67). In the orthostatic phase, BP drops rapidly and instantly within a few seconds due to the lack of venous return and the concomitant decrease in SV, and it rebounds to normal

owing to the baroreflex mechanism, which initiates vasoconstriction and thereby greatly increases the total peripheral pressure (TPR) within 10 to 20 s in healthy subjects (67, 68). For this rebound of BP, the increase in TPR has much greater importance than CO change (69–72), which results in a great increase in DBP and relatively small change in PP, thereby increasing SBP in almost the same degree as DBP. Therefore, we regarded the BP change period when BP rebounds by the unloaded baroreceptors, initiating the increase in TPR, as the DBP−dominant−BP change.

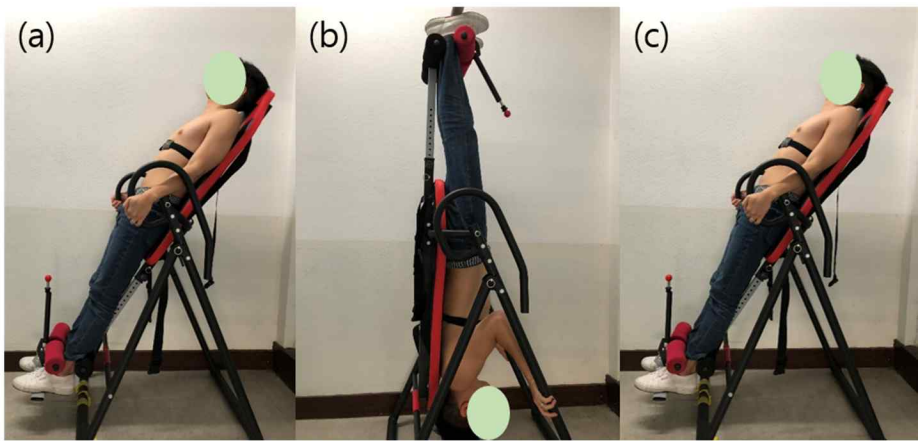

Figure 3.2 Subject on the tilting machine. First, for 3 min, the subject was in (a) head−up position, followed by (b) head−down tilt by −90° for 3 min and (c) returned instantly to upright position.

In the second stage, to assess the model when generalized to new subjects, the group model from the first study was build. Then, extra subjects were asked to cycle in the same way as done in the first study. There are two reasons for not involving the orthostatic stress intervention in this stage. First, as the purpose of the second stage is to verify the generalization ability of the model, which complements the performance when two BPs are not highly correlated, the DBP dominant BP change intervention was thought to be not necessary. Secondly, orthostatic stress may cause faint and discomfort to certain subjects, which lowers their participation and makes it difficult to validate the model against the general population, especially for subjects who are relatively old.

At the final stage, the developed device was attached in the same way as was done in the indoor studies and, for reference BP, the subjects were asked to wear a portable ABPM (ABPM 7100; Welch-Allyn, US), which consists of a cuff designed to wrap around the upper arm, and a main head, which controls the cuff and records the data and is designed to hang across the body (Fig. 3.3). The ABPM was set to automatically measure BP twice per hour during daytime and once per hour during nighttime. The

signals, estimated BP, and reference BP were recorded via the developed android-base mobile application during a daily activity of as long as 24 h, including the sleep period.

Figure 3.3 Setup of daily BP monitoring. Subjects wore the developed device and reference oscillometric method-based ABPM, carrying the mobile phone that collects the data, shows processed signals, and estimated BP online. They were asked to behave freely during a day, without particular regulations on any type of activity.

3.2.4 Data Collection

After placement of the device, subjects were instructed to cycle (Fig. 3.1) for 10 min with 3 min of rest and 5 min of a recovery phase prior to and after the exercise. During cycling, the same intensity of the exercise was applied to all subjects, but in some cases when the BP change was minimal, the intensity was increased by a change in the speed and pedaling load. Following the exercise protocol, the subjects were laid on a head-up/down tilt machine (Fig. 3.2). In the beginning, the subjects were in head-up positions for 3 min, then the machine was tilted down to −90° to obtain a subject upside down posture for 3 min. After the head-down position, the machines returned to the upright position instantly to induce orthostatic stress and were held for 5 min. During the protocol, PPG, SCG, and ECG from the device and reference BP were acquired continuously by the developed data acquisition PC program.

For data in the first and second stage, we extracted the BP-related parameters (PAT, PEP, PTT, and SA) as described in Chapter 2 for each subject record. Each BP level (SBP, DBP, and PP) was calculated in the same length of window (10 s) as

performed for other parameters in the “Signal processing” section in Chapter 2. In every window of 10 s, sliding by 2 s, the highest peaks and lowest troughs of BP waveform were detected and averaged, for SBP and DBP, respectively. PP was calculated by the difference between the averaged SBP and DBP. For each cycling subject, we extracted five pairs of BP−related parameters (PAT, PEP, PTT, and SA) and BP values (SBP, DBP, and PP) in the rest and exercise phases by evenly segmenting the phases and averaging them over the segmented period, respectively, to minimize noise. This resulted in a total of 10 pairs of datasets for each subject in the cycling protocol. In the case when BP rose rapidly during the exercise, which often caused error in the BP measurement device, and SBP increased excessively, exceeding more than 35 mmHg compared to that in the rest phase, five pairs were obtained instead in the recovery phase, in the same way as in the other phases, before BP returned to baseline. For each subject in the HDU protocol, the same number of datasets (N=10) from the cycling protocol was obtained in the interval between the point when BP dropped to a minimum by HDU change and the point when BP returned to baseline. Finally, a dataset comprising a total of 20 pairs of BPs

and the parameters was obtained from each subject involved in the first stage.

For the second stage, one calibration point was extracted from the first half of recording in the rest phase, and three pairs of BPs and BP related parameters were extracted in the rest of the rest phase and exercise phase, respectively, in accordance with the IEEE standard.

For the final stage, the subjects involved in this stage were asked to behave freely during a day without particular regulation on the type of activity. It was only asked that when the reference device measures BP, they should stay as still as possible because movements considerably affect the reliability of a reference BP value. It was notified that the subjects could take off the device as they wanted, such as when they took a shower or did excessive exercise (e.g., weight training, running). The time when the study began was different by subject depending on their preferences. The ABPM was set to automatically measure BP twice per hour during daytime and once per hour during nighttime. The BP-related parameters calculated as explained in Chapter 2 were averaged over 6 min each time the reference BP

was measured by the ABPM device (3 min prior to and after BP measurement). In 6 min, if less than half of the parameters were acquired owing to low signal quality of either PPG, SCG, or ECG, a pair of the measured BPs and parameters at that time stamp was discarded.

Pairs of the parameters and reference BPs acquired within an hour were averaged to minimize error in the reference BP measurement, as it was often measured in a bad posture or with motion artifacts, which may increase its unreliability. For example, if two pairs of the parameters and reference BPs were acquired at 14:00 and 14:30, respectively, they were averaged, which resulted in one pair of BP parameters and reference BPs for every hour. Because the daily pattern varied between subjects, and thereby the number of discarded data pairs owing to low quality of signal was different by subject, the number of collected datasets per subject was not the same.

3.2.5 Data analysis

First, we assessed the changes in BP-related parameters (PAT, PTT, PEP, and SA) and BPs in each protocol. For the cycling protocol, five pairs of the parameters and BPs were averaged over the rest phase and exercise phase and regarded as baseline and perturbed values, and the group average difference between the two values was compared. For the HDU protocol, the early five pairs and late five pairs were considered as perturbed values and baseline values, respectively, and the group change was compared. In all these comparisons, the paired t-test was used with a significance level of $p < 0.05$. The correlation between time features (PAT and PTT) and BPs (SBP and DBP) in each protocol and the two protocols combined for each subject were also analyzed in terms of Pearson's correlation coefficient.

Next, we also calibrated the proposed model and other univariate models using PTT or PAT to each reference BP for each subject. Then, we computed the mean absolute difference (MAD) and correlation between each calibrated BP and reference BP for all subjects. The definition of MAD will be explained in the following

section. The MAD from the models was compared using the paired t-test. We used a significant level of p-value < 0.05. Likewise, SA was calibrated to the reference PP, and the MAD and correlation was computed.

Table 3.1 Proposed model and other comparative models. The models marked with an asterisk (*) are the models for SBP and DBP proposed in this study.

Models for SBP		Models for DBP	
1	$a \cdot PTT + b$	1	$a \cdot PTT + b$
2	$a \cdot PAT + b$	2	$a \cdot PAT + b$
3	$a \cdot \ln PTT + b$	3 *	$a \cdot \ln PTT + b$
4	$a \cdot \ln PAT + b$	4	$a \cdot \ln PAT + b$
5 *	$a \cdot \ln PTT + b \cdot SA + c$		

In order to assess the generalization ability of the model, we derived optimal model coefficients from the subject group in the first study and applied them to the new subject group. The detailed process of deriving optimal models is as follows.

Using all different combinations of coefficients from 0 to 100 for b and −100 to 0 for a in eq. 9, we calculated the minimum mean squared error for each subject and summated the mean squared errors from all subjects. When we calculated the minimum mean squared error for each subject, constant c in eq. 9 was considered a subject dependent variable as c will be replaced with a calibrated value in real practice. Thus, c was fitted to each subject dataset with the given pair of coefficients. We selected the pair of coefficients that minimized the summated mean squared errors for all subjects as the optimal model coefficients. This work was repeated for the search of the optimal model coefficient a' for DBP in eq. 10.

The optimal model was applied to the new subjects' datasets, calibrating the model using one extra pair. Further, we calculated the MAD and correlation between the estimated and reference BP for all datasets from all subjects. In addition, the MAD was

calculated for two groups of datasets: the static and dynamic groups. The static group dataset consists of the three pairs of estimated and reference BPs after calibration and before the intervention for each subject, and the dynamic group dataset comprises the three pairs of estimated and reference BPs after the induced BP change.

In order to assess the BP estimation performance during a daily activity, the BP estimation model equipped with optimal coefficients derived in the second stage was applied to each subject with one-point measurement for calibration. Among the acquired datasets, the data point considered the most reliable and measured in the most stable condition was selected for calibration. Using the calibrated model, we estimated BPs and computed the MAD with reference BPs for each subject and the average of MAD values from all subjects was evaluated according to the IEEE standard. In addition, the estimated and reference BPs from all subjects were pooled and correlation coefficients between them were analyzed for SBP and DBP, respectively.

3.2.6 Evaluation standard

The most widely used standards to evaluate the performance of BP estimation are the Association for the Advancement of Medical Instrumentation (AAMI) standard (73) and the British Society of Hypertension (BSH) standard (74). The AAMI standard requires a mean error of less than 5 mmHg and a mean standard deviation of less than 8 mmHg to pass the standard. The BHS standard defines grades in four levels (A/B/C/D), and to meet the A grade, more than 60% of the measurement errors should be less than 5 mmHg, 85% less than 10 mmHg, and 95% less than 15 mmHg. However, those standards may not be appropriate for cuffless BP estimation, which is a continuous measurement and generally requires a calibration process, as they do not cover all aspects needed for the cuffless BP measurement technique (75). Given that those conventional standards do not require change in BP for an individual, the performance of the cuffless BP measurement methodology, which at least measures and uses one point of reference BP, may be overrated if one's BP does not vary from the reference BP at the calibration point.

Recently, with the emerging developments of cuffless blood pressure techniques, there is an increasing need for a valid standard for cuffless blood pressure measurement. The IEEE Engineering in Medicine and Biology Society has published the standard for wearable, cuffless blood pressure measuring devices. It is distinguished from other conventional standards in that it requires the report of BP change distribution from the calibration point and the report of performance by different BP change levels. Therefore, one can find whether the BP change is not induced sufficiently to cover the requisite range (up to 30 mmHg for SBP), which might result in overestimation of the performance. As a validation criterion, it suggests using MAD. Here in the thesis, MAD will be used as the main criterion and is calculated as follows:

$$\mathrm{MAD}=(\sum_{i=1}^{n}|p_i - y_i|)/n, \tag{11}$$

where p_i is the estimated or measured BP from the device, y_i denotes the reference measurements of BP, and n is the data size (75). It grades the performance by MAD in four levels. MAD of less than 5 is regarded as grade A, less than 6 as B, less than 7 as C, and more than 7 as D. For the initial phase of

study, MAD less than 7 is regarded acceptable to move forward to a subsequent study. The grade given by the IEEE standard is not always corresponding with that determined by the conventional standard, depending on the error distribution. For details of the comparison with the conventional standards, see (75).

3.3. RESULTS

3.3.1. Changes in parameters and BPs in different protocols

Figure 3.4 shows the changes in BP-related parameters and BPs with respect to the baseline in each protocol. In cycling, PP increased greatly compared to DBP (PP increased by 38.19 ± 12.76% and DBP increased by 10.71 ± 15.46%). The difference in BP between the baseline and perturbed values was significant. The BP-related parameters all changed in the opposite direction of BP. PTT and PEP decreased by 28.87 ± 16.58% and 18.74 ± 9.28%, respectively, and PAT, the sum of two, decreased by 23.78 ± 8.58%. SA showed a marked increase by 99.92 ± 71.79%. The difference in the parameters between the baseline and perturbed values were significant. In the HDU protocol, SBP and DBP increased by 9.84 ± 6.56% and 26.58 ± 16.96%, respectively, whereas PP slightly decreased by −8.70 ± 6.90%, which shows dominant changes in DBP compared to PP. The difference between the baseline and perturbed values was significant for all BPs. PTT decreased by 12.70 ± 7.65%, as it

did in the cycling protocol, while PEP increased by 8.50 ± 5.46%, which was a different direction compared to that of the cycling protocol. PAT marginally decreased by 3.07 ± 5.07%, and it showed the same direction as in the cycling protocol, but its amount of change was very different in the two protocols. SA showed a slight increase by 5.76 ± 18.76%. The difference between baseline and perturbed values was significant in PTT and PEP, but insignificant in PAT and SA. It was PTT that changed the most consistently with BP in the two protocols. Table 3.2 presents the group mean and standard deviation of values of the BP-related parameters and BPs in the baseline and perturbed states for each protocol.

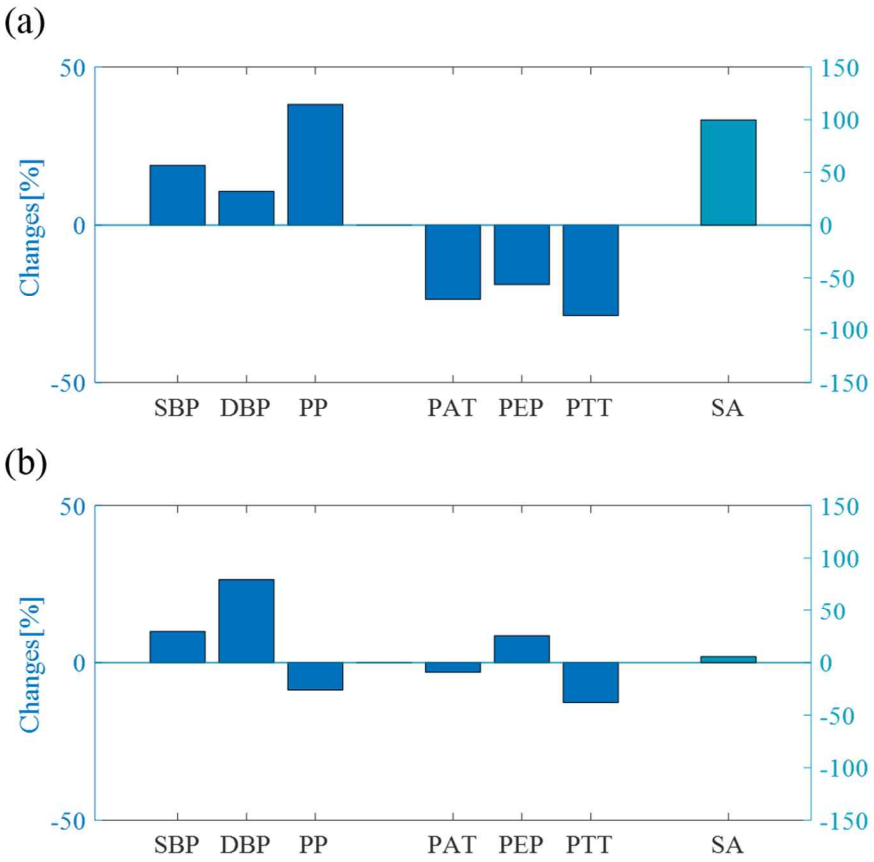

Figure 3.4 Changes in BP-related parameters and BPs. Changes in BP-related parameters and BPs with respect to (a) the rest phase in the cycling protocol and (b) beginning of the head-down to up change.

Table 3.2 Comparison of the parameters and BPs in two protocols. The group averaged value of the parameters and BPs before exercise (BE) and after exercise (AE) was calculated, along with the changes in values in AE with respect to BE. The group averaged value of the parameters and BPs before reflex (BR) and after reflex (AR) was calculated, along with the changes in values in BR with respect to BE. The asterisk (*) indicates a significant difference between the two states ($p < 0.05$).

	Cycling			Head down/up		
	BE	AE	Changes [%]	BR	AR	Changes [%]
SBP [mmHg]	118.12 ±11.56	139.88 ±9.26	18.91 ±7.19 *	106.94 ±14.24	116.95 ±12.05	9.84 ±6.56 *
DBP [mmHg]	78.62 ±15.07	85.64 ±12.02	10.71 ±15.46*	60.41 ±15.32	74.57 ±12.25	26.58 ±16.96 *
PP [mmHg]	39.49 ±7.44	54.24 ±9.78	38.19 ±12.76*	46.53 ±8.94	42.38 ±8.09	-8.70 ±6.90 *
PAT [ms]	150.39 ±17.93	115.37 ±23.59	-23.78 ±8.58 *	149.49 ±16.81	144.81 ±17.08	-3.07 ±5.07
PEP [ms]	81.15 ±13.30	65.00 ±5.89	-18.74 ±9.28 *	69.48 ±6.90	75.42 ±8.90	8.50 ±5.46 *
PTT [ms]	69.04 ±19.96	50.65 ±21.69	-28.87 ±16.58 *	80.01 ±14.02	69.39 ±10.32	-12.70 ±7.65 *
SA [au]	0.0080 ±0.0053	0.0160 ±0.0130	99.92 ±71.79*	0.0095 ±0.0070	0.0098 ±0.0069	5.76 ±18.76

3.3.2. Comparison between PTT and PAT

Figure 3.5 shows the correlation between time parameters (PAT and PTT) and BPs in each protocol and the two protocols combined. In the cycling protocol (Fig. 3.5a), the correlation coefficients of PTT with DBP and SBP were −0.61 ± 0.28 and −0.76 ± 0.20, respectively, while those of PAT with DBP and SBP were −0.64 ± 0.29 and −0.94 ± 0.05, respectively. PTT and PAT showed a similar correlation with DBP, and no significant difference was found, while PAT showed greater correlation than PTT for SBP. This may be attributed to the PEP, which shows a sensitive response during exercise and moves in the same direction with PTT, and thus, causes larger absolute changes in PAT than those in PTT. In contrast, for the HDU protocol (Fig. 3.5b), when DBP dominated the change in BP, the correlation coefficients of PTT with DBP and SBP were −0.73 ± 0.17 and −0.62 ± 0.20, while those of PAT with DBP and SBP were −0.47 ± 0.51 and −0.38 ± 0.47. The correlation of PTT with DBP was significantly higher than that of PAT with DBP. PTT showed a similar correlation between the two protocols, whereas PAT varied greatly in the HDU protocol. PAT often

showed a contrary correlation, resulting in great variance in DBP and SBP. This may also be attributed to the effect of PEP, which showed a different relationship with BP between the cycling and HDU protocol. In the HDU protocol, PEP increased when DBP and SBP increased, while PTT decreased as it did in the cycling protocol. Consequently, the change in PAT was cancelled by the sum of contrary changes in PTT and PEP, which resulted in an inconsistent relationship of PAT with BPs and greatly lowered the correlation coefficient with BPs as compared to PTT.

Figure 3.5c also shows the correlation for the pooled datasets from two different protocols. The correlation coefficients of PTT with DBP and SBP were -0.72 ± 0.13 and -0.80 ± 0.11, respectively, while those of PAT with DBP and SBP were -0.54 ± 0.25 and -0.81 ± 0.14, respectively. PTT was significantly more correlated with DBP than PAT, as it was in the HDU protocol. PAT and PTT showed a similar correlation with SBP, and the difference was not significant. This may be explained by the fact that the BP change was greater in the cycling protocol than in the HDU protocol, which may render the relationship between PAT and SBP in the cycling protocol more pronounced in the pooled datasets. Thus, PAT showed a stronger relationship

with SBP than PTT, although PAT often showed an opposite relationship with SBP in the HDU protocol, whereas PTT showed greater correlation with DBP than PAT because, compared to PAT, PTT consistently exhibited a higher correlation with DBP in all protocols.

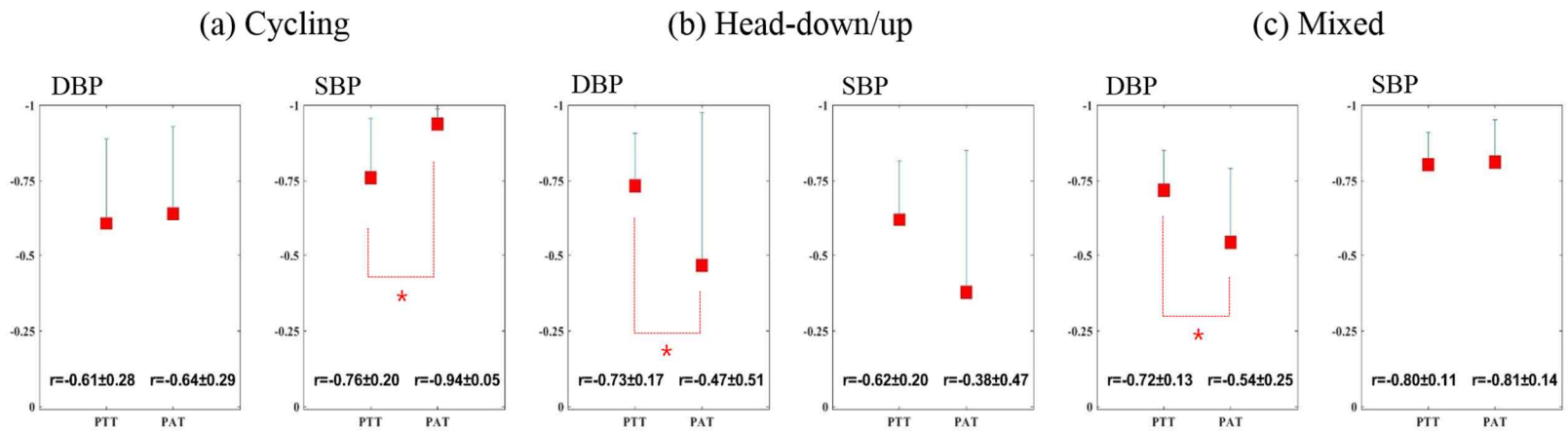

Figure 3.5 Correlation between BPs and PTT/PAT. The correlation between time features (PAT and PTT) and BPs was compared in the (a) cycling and (b) HDU protocols, and (c) in the two protocols combined. The asterisk (*) indicates a significant difference ($p < 0.05$).

3.3.3. Efficacy of the proposed model

The proposed model (model 5 for SBP and 3 for DBP) was calibrated to the reference BP to obtain subject-specific coefficients and the difference between the calibrated BPs and the reference BP was computed. In the same way, the performance of other models, including the widely used linear and logarithmic models using PTT or PAT as a sole parameter (model 1 ~ 4), was compared. The performance between the linear model and logarithmic model was quite similar when using the same parameter (between models 1 and 3 and models 2 and 4). Thus, the proposed model for SBP (model 5) was compared to the logarithmic models (3 and 4) for a more equivalent condition and model for DBP (model 3) was compared to the counterpart PAT model (model 4).

Figure 3.6 shows the comparison between the proposed model and other comparative models using PTT or PAT for the dataset from each protocol and for the dataset from the two protocols combined. Regarding the performance of the SBP estimation, a contrary performance of PTT and PAT in the two different types of intervention was clearly found. In the cycling protocol, the

MAD when using PTT or PAT was of 7.00 and 6.37, respectively, showing better performance of PAT, although it was not a significant difference. On the contrary, the MAD of the proposed model was 5.09, showing a markedly better performance than that of the models using only PTT or PAT (27% and 20% of decrease with respect to the two counterparts, respectively). In the HDU protocol, the MAD when using PTT or PAT was of 5.01 and 5.86, respectively, which was a reversed result compared to that of the cycling protocol, showing better performance of PTT with a significant difference. Meanwhile, the MAD of the proposed model was 4.05, showing smaller errors than those of the models using only PTT or PAT (19% and 31% of decrease with respect to the two counterpart models, respectively). When two datasets from the two protocols were combined, the MAD of PTT and PAT was of 6.01 and 6.11, respectively, showing a similar level without significant difference, whereas the MAD of the proposed model was 4.57, showing a superior performance than that of the other two counterparts by a great margin (24% and 25% of decrease with respect to the two counterpart models, respectively). The overall performance of the proposed model

met the requirements for grade A (MAD < 5 mmHg) of the IEEE standard.

In terms of the DBP estimation performance, the MAD of PTT for the cycling datasets, HDU datasets, and combined datasets from the two protocols, was of 6.15, 5.64, and 5.89, respectively, and that of PAT was of 6.88, 7.04, and 6.96, respectively. PTT showed consistently better results than PAT in all types of datasets. The overall performance of the logarithmic model using PTT met the requirements for grade B (MAD < 6 mmHg) of the IEEE standard.

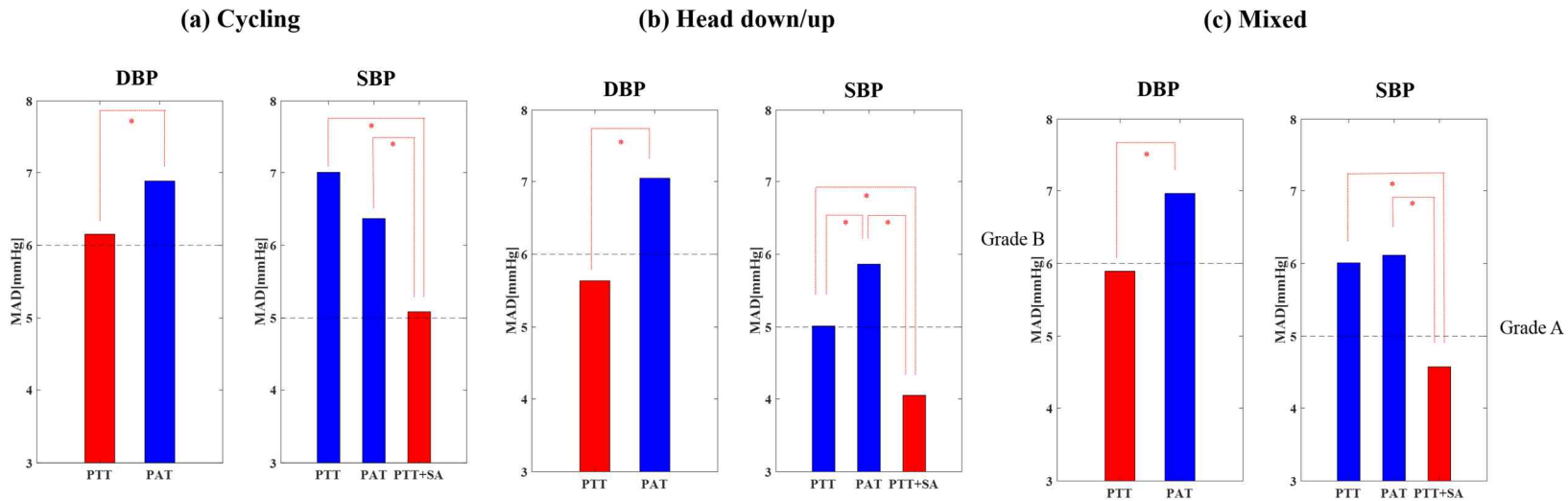

Figure 3.6 Performance comparison between models. The proposed model and other two logarithmic models using PTT or PAT for the dataset from (a) the cycling and (b) HDU protocols, and (c) the two protocols combined (mixed) were compared. The dash line represents the grade A and grade B level for SBP and DBP, respectively. The asterisk (*) indicates a significant difference ($p < 0.05$).

Figure 3.6 and 3.7 show the correlation and Bland–Altman plots for the proposed model versus SBP and DBP. The proposed model, incorporating SA into the PTT model, yielded an excellent correlation ($r = 0.93$) with SBP. The DBP estimation model, mostly adhering to a theoretical basis, also showed a tight correlation with the reference DBP ($r = 0.86$). The Bland–Altman plot verified that the variance of error was not biased, and most of the errors were within the limit of agreement, except for a few.

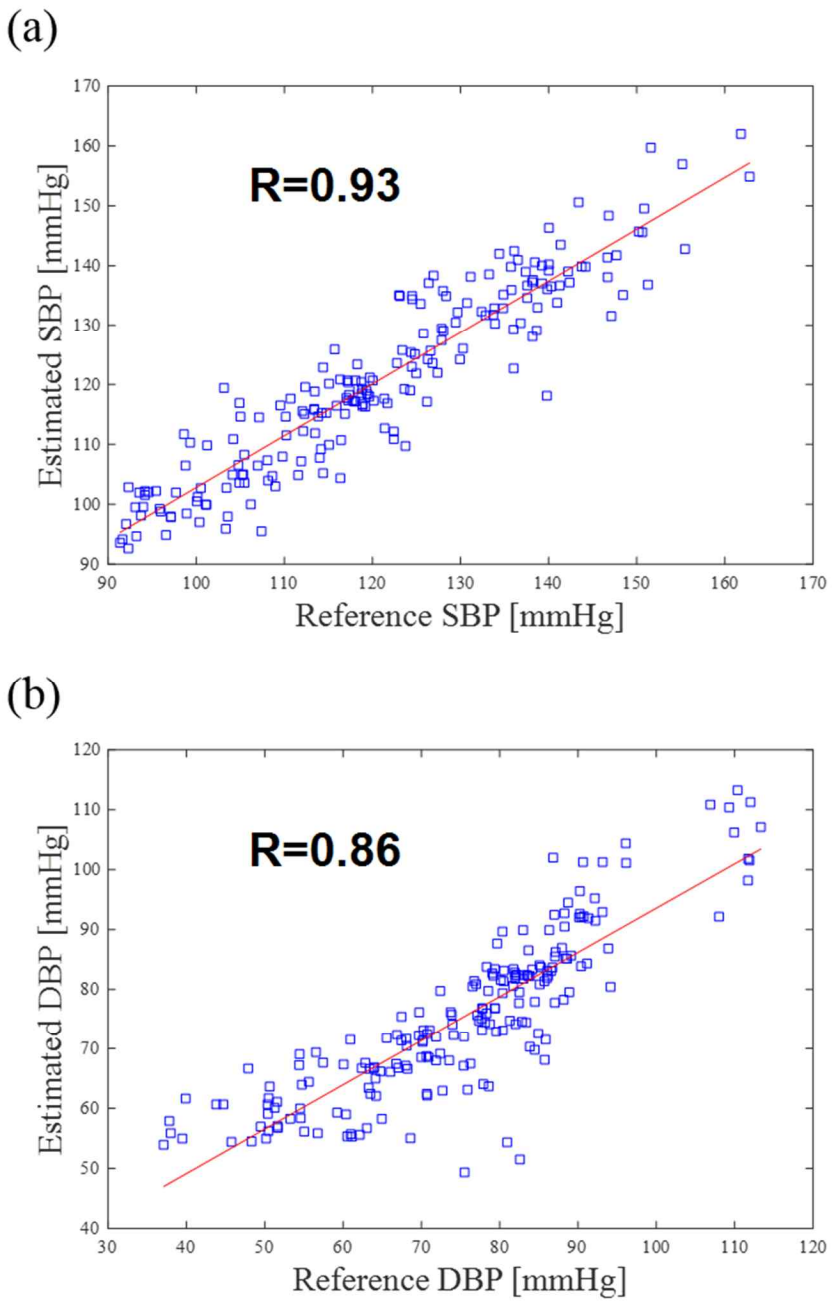

Figure 3.7 Correlation plots for estimated BPs by the proposed model versus (a) SBP and (b) DBP.

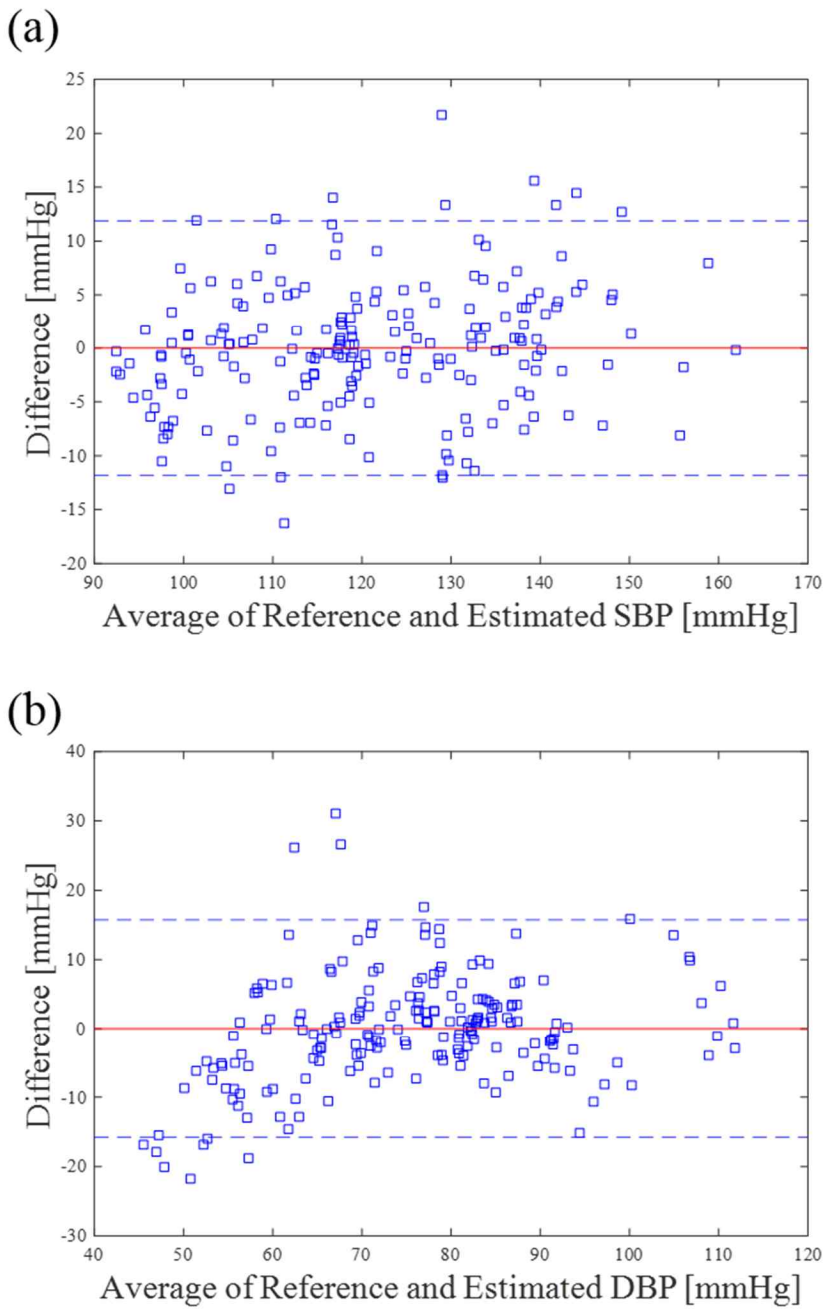

Figure 3.8 Bland–Altman plots for estimated BPs by the proposed model versus (a) SBP and (b) DBP.

Figure 3.8 shows the correlation and Bland-Altman plots for the calibrated PP using only SA versus the reference PP in order to assess the effect of SA as an indicator of PP. The correlation coefficient was 0.91, and most of the errors were also within the limit of agreement, which supports the guess that SA can be a potential marker of PP.

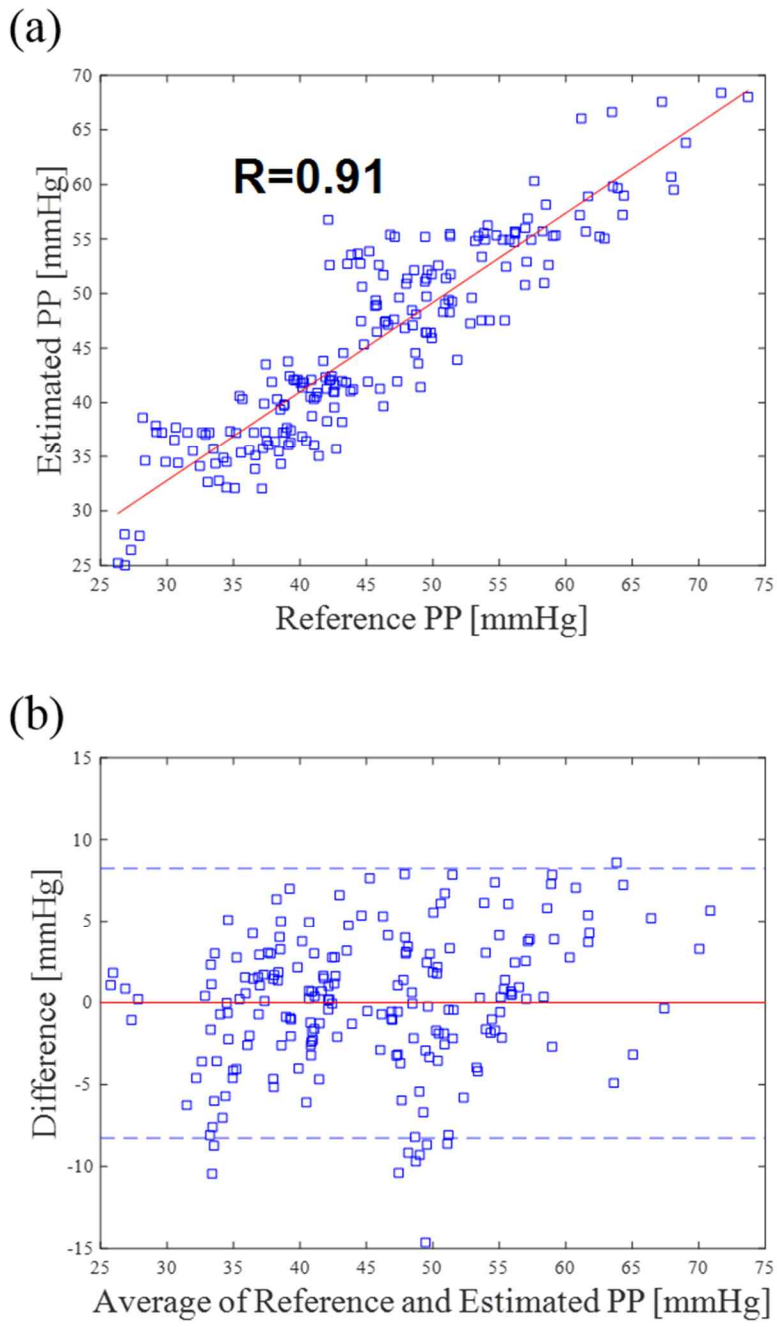

Figure 3.9 Correlation and Bland–Altman plots for the estimated PP by

SA versus reference PP.

3.3.4. Generalization ability

It was found out that the optimal coefficients of a, b for SBP, and a' for DBP for the previous subject group were −20.04, 10.42, and −18.24, respectively (Fig. 3.9). Table 3.3 presents the overall performance according to the IEEE standard when generalized to unseen new subjects. The overall MAD was of 6.89 for SBP and 3.66 for DBP, which is acceptable level for IEEE standard. As the IEEE standard recommends, the accuracy at different BP change levels is shown along with the accuracy at the static level, where the BP change was not induced. The MAD at different BP change levels was greater than the overall accuracy, and the static level was lower than the overall one, as could be anticipated. Figure 3.10 shows the distribution of the induced BP change as the IEEE standard requires. The induced SBP change was great, ranging up to 40 mmHg, and it was largely distributed between 15 to 35 mmHg. The ratio of number of data between 0–15 mmHg of BP changes and 15–30 mmHg of BP changes was approximately 56:44, similar to the IEEE standard,

while the induced DBP change was narrow and mostly of less than 10 mmHg. Thus, it might result that the performance of the DBP estimation appears to be relatively better than that of the SBP estimation.

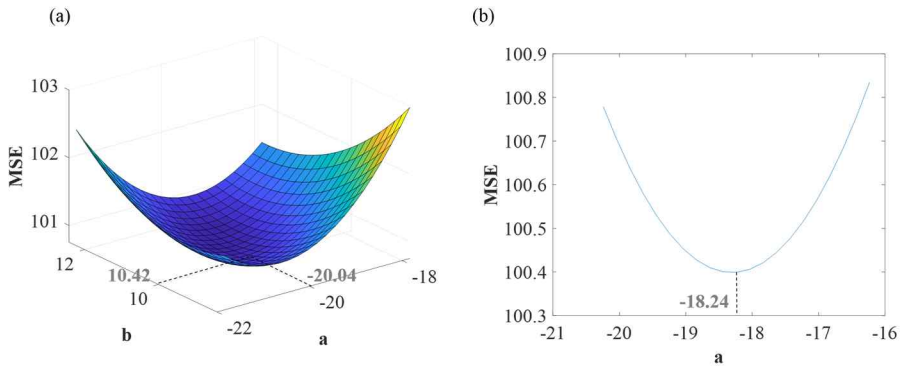

Figure 3.10 Optimization of model coefficients. Using all different combinations of coefficients from 0 to 100 for *b* and −100 to 0 for *a* in eq. 20, we found the optimal pair that minimized the overall error of SBP estimation for the subject pool in the first study. This work was repeated for the search of the optimal model coefficient *a'* in eq. 21 for DBP.

Table 3.4 presents the subject demography. There was one subject whose entry BP range was within stage 1 hypertension level, 8 pre-hypertensive subjects whose entry SBP were in between 120-140 and DBP in between 80-89, and normotensive subjects whose entry SBP was less than 120 and DBP less than

80. The age of the subjects was relatively more diverse than the subject pool for study 1, ranging from 25 to 54, and the mean/standard deviation was of 32.35 ± 7.96.

Table 3.3 Overall performance according to IEEE evaluation standard. MAD was calculated for different BP levels before and after BP change was induced along with mean difference (MD)/ Standard deviation (SD) and Cumulative percentage (CP) of 5/10/15%, which are criteria by AAMI and BHS, respectively.

	SBP						DBP					
BP changes	MAD	MD	SD	CP5	CP10	CP15	MAD	MD	SD	CP5	CP10	CP15
Static test	4.05	0.18	5.54	68.33	96.67	98.33	2.50	0.16	3.63	90.00	98.33	98.33
BP change induced	9.73	6.43	9.00	18.33	50.00	83.33	4.81	-0.53	6.22	61.67	90.00	96.67
Total	6.89	3.31	8.07	43.33	73.33	90.83	3.66	-0.18	5.08	75.83	94.17	97.50

Table 3.4 Subject demography.

Total number		**20**
Entry BP range	Normal	11
	Prehypertension	8
	Stage 1 hypertension	1
	Stage 2 hypertension	0
Age	Me/std	30.15/4.41
	Range	25~40

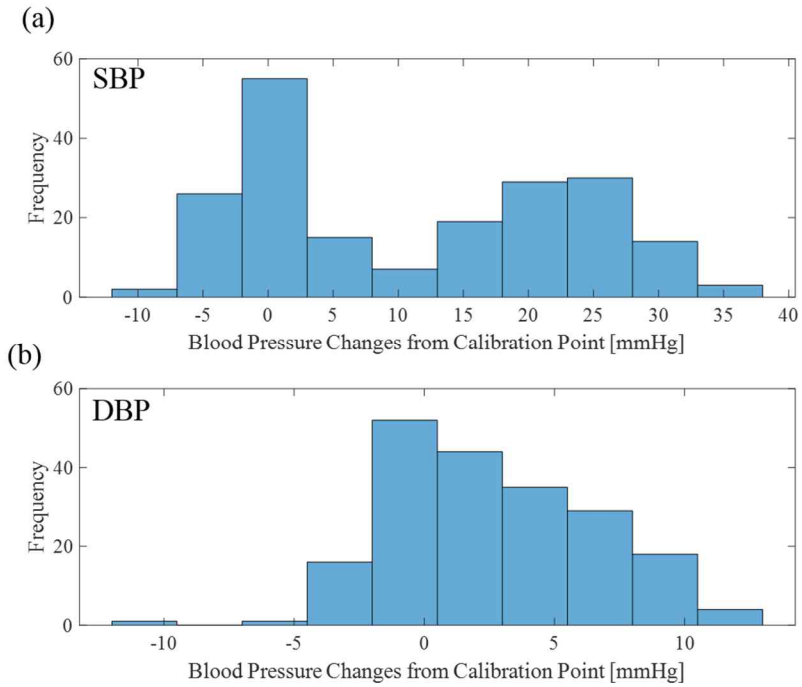

Figure 3.11 Distribution of induced BP change. (a) The induced SBP change was great, ranging up to 40 mmHg, and was largely distributed between 15 to 35 mmHg. (b) The induced DBP change was narrow and

was mostly of less than 10 mmHg.

Figure 3.11 and 3.12 show the correlation and Bland-Altman plot between the estimated and reference BPs. The correlation coefficient between the estimated and reference SBP was 0.88 and between the estimated and reference DBP was 0.86, which showed a tight correlation between the estimated and reference BPs, but lower than the correlation when using subject-specific coefficients. The correlation of SBP was slightly higher than that of DBP, although it may be attributed to the fact that the DBP change was smaller than the SBP distribution, which generally reduces the correlation coefficient and estimation error (Fig. 3.11). The Bland-Altman plot indicates that the estimation errors were slightly positive-biased for SBP. As SBP increases, the errors tended to be more positive-biased, while as SBP decreases, the errors tended to be less biased. This tendency was not found in DBP, although a few errors were lower than the negative line of agreement. Overall, except for a few points, most of the errors were within the line of agreement (Fig. 3.12).

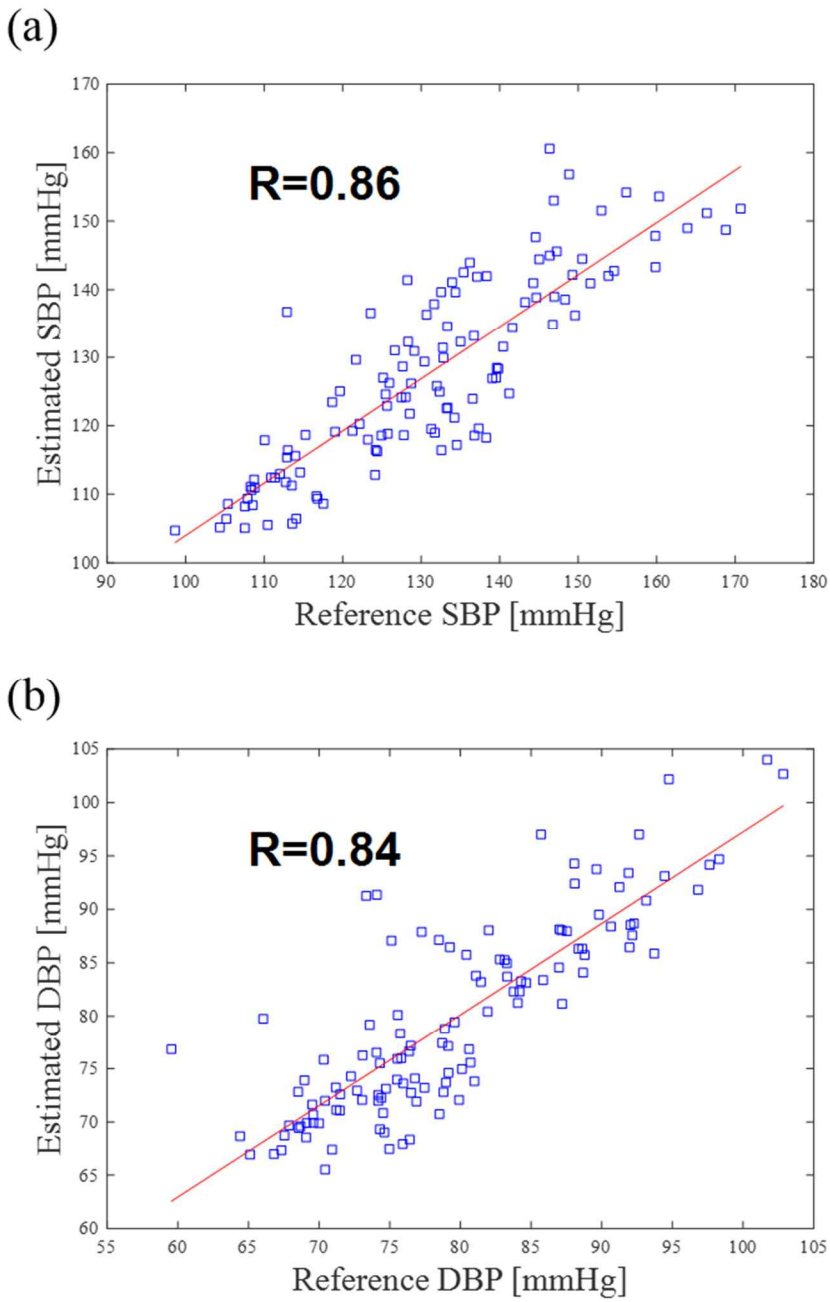

Figure 3.12 Correlation plots between estimated BPs by the proposed model versus reference (a) SBP and (b) DBP.

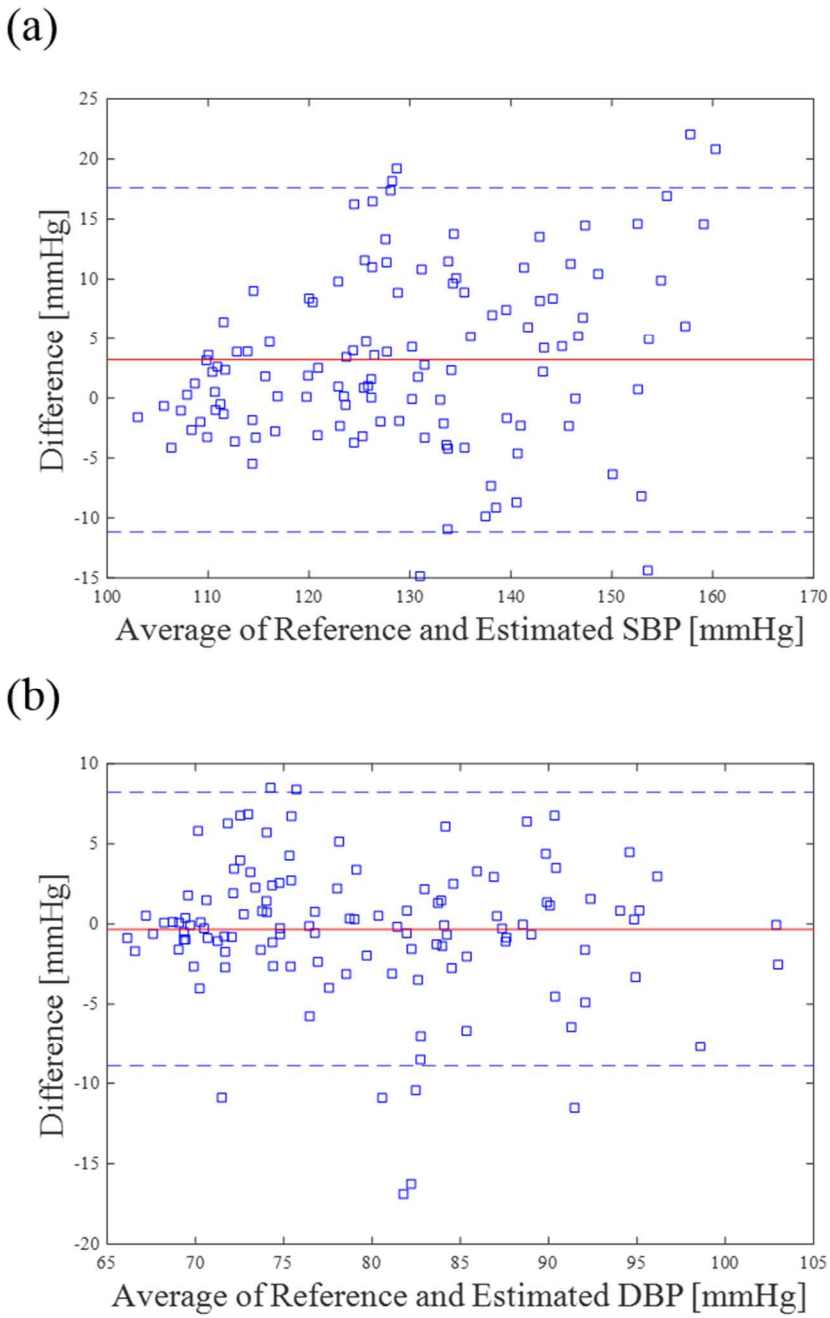

Figure 3.13 Bland–Altman plots for estimated BPs by the proposed model versus reference (a) SBP and (b) DBP.

3.3.5. Daily monitoring

Nine subjects participated in the daily monitoring stage. However, data from three subjects could not be used as less than half of the measurements were acquired, mainly owing to connection failure with the mobile application and signal degradation from excessive movements. More than 20 h of data were acquired from four subjects, and 17 h and 16 h of data were acquired for subject 3 and subject 5, respectively.

Figure 3.14 shows the typical trend of change in the reference (green boxes) and estimated (red line) BP by the proposed model during a day from subject 2. It should be noted that a nocturnal drop and a slight morning surge were captured by the proposed BP monitoring system.

Figure 3.15 shows the correlation and Bland–Altman plot for the estimated and reference BP. The correlation coefficients of SBP and DBP were 0.77 and 0.67, respectively. These values were much lower than the correlation coefficients from previous stages of study, which may be attributed to various reasons, including the fact that the signal quality in daily life may be obviously worse than that in controlled settings and the fact that

the BP change was considerably limited in daily life, which lowers the correlation coefficient in general. The correlation coefficient of DBP was less than that of SBP, which may be explained by the fact that the personal variation of DBP was much less than that of SBP, which results in a narrow distribution of DBP in the pooled datasets.

Table 3.5 presents the individual and overall performance of BP estimation during daily monitoring. The MAD for SBP and DBP was of 5.87 and 5.63, respectively, which satisfies grade B according to the IEEE standard. During a day, approximately 30 mmHg of change was found in both SBP and DBP, which strengthens the necessity of daily BP monitoring.

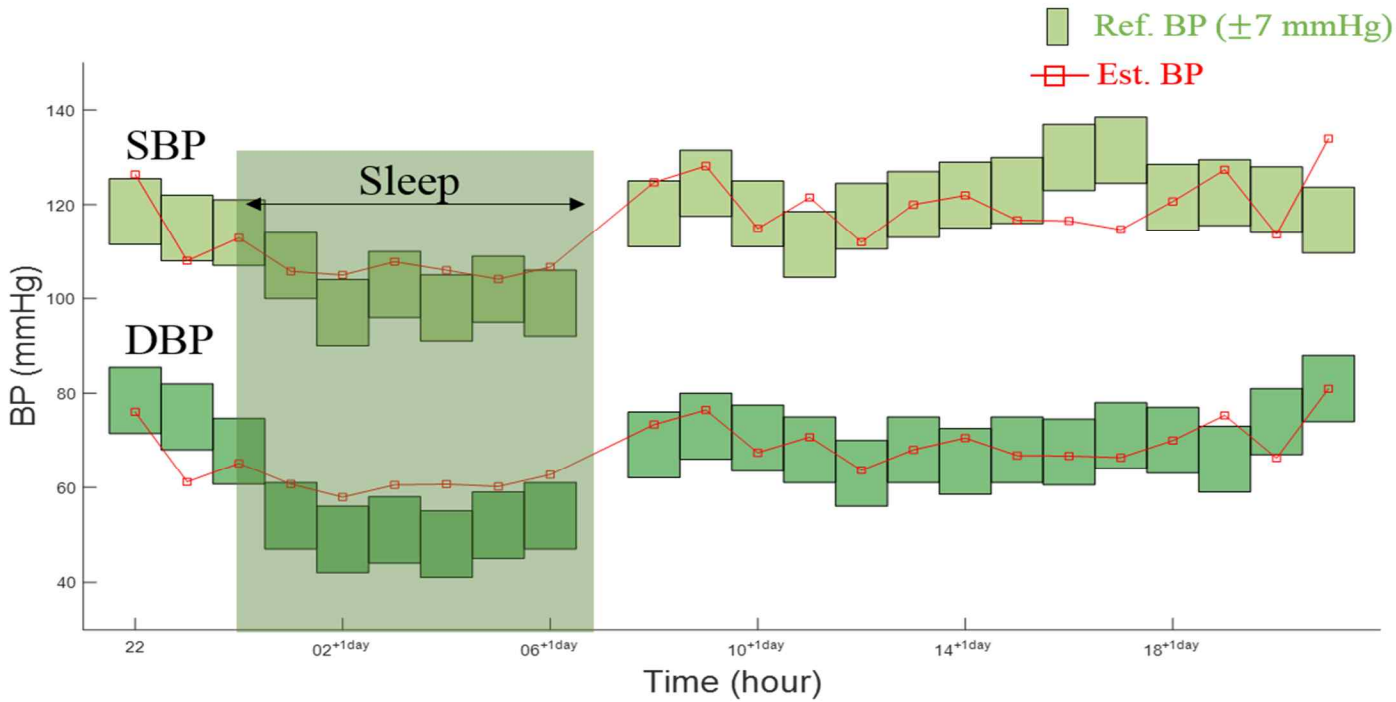

Figure 3.14 Typical trend of change in the reference and estimated BP during 24 h. The reference BP was indicated by green boxes with ± 7 mmHg of difference with the true value. The estimated BP by the proposed model is shown with the red line.

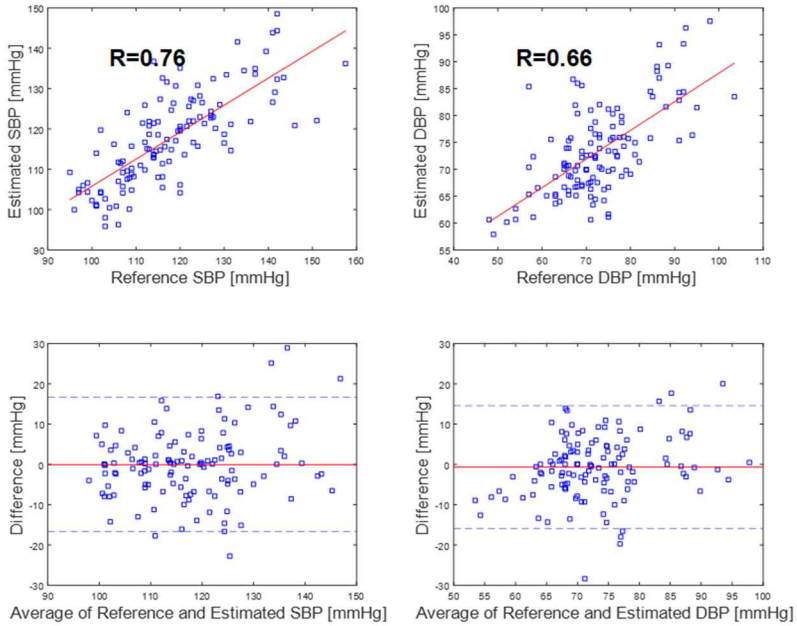

Figure 3.15 Correlation and Bland–Altman plot between estimated BPs and reference BPs.

Table 3.5 Individual and overall performance of BP estimation in daily monitoring.

Subject	SBP		DBP	
	MAD	Range	MAD	Range
1	9.41	112-157.5	8.44	57-103.5
2	6.08	97-131.5	5.26	48-84.5
3	3.77	105-131.5	4.90	66-81
4	4.33	97-124	5.70	57-85
5	6.74	113-151	4.36	57-76
6	5.94	95-120	5.58	58-82
Overall	**6.04 ± 1.99**	103.17-135.92	**5.70 ± 1.42**	57.17-85.33

3.4. DISCUSSION

3.4.1. Summary

In this chapter, we sought to assess the efficacy of the proposed model, which incorporates a new indicator into the conventional PTT-based model. We compared the proposed and conventional models using PTT or PAT in two contrary interventions. Furthermore, we validated the proposed model for the general population and in daily life to demonstrate its potential of real use. The results suggested that (1) the proposed model, which employed SA in conjunction with PTT for SBP estimation, outperformed the conventional univariate model using PTT or PAT (Fig. 3.6), and therefore, enabled independent estimation of SBP and DBP, which can often show different movements; (2) for practical use, the proposed model showed potential to be generalized (Table 3.3) beyond subject-specific model fitting; and (3) the proposed model and system demonstrated the potential of continuous BP monitoring in daily life (Fig. 3.13) without any intervention of users or regulations.

3.4.2. Comparison between PTT and PAT

PAT is the sum of PEP and PTT, which are affected by different cardiovascular mechanisms. PTT, which is the pure vascular transit time, is the one associated with BP based on the vessel wall property. In contrary, PEP is affected by various factors, including cardiac contractility, preload, and afterload (76, 77). Thus, if PTT and PEP show conflicting movements in cases such as when there is an increase in afterload expressed by an increase in DBP, which accordingly shortens PTT and at the same time increases PEP (77), the change in PAT could be cancelled out by the different direction of change in PTT and PEP, and thereby it would not be well correlated with BP. It was found in this study that PEP showed different change with PTT (see Fig. 3.4) and the correlation of PAT with BP was highly degraded accordingly (see Fig. 3.5) when the afterload was perturbed, a result that is consistent with previous studies (34, 78) and the theory. However, it was also observed that PAT was substantially correlated with SBP (see Fig. 3.5), significantly more than PTT in the cycling protocol, which was also often reported and has not been well understood in previous studies

(38, 63, 64, 79–81). This may result from two reasons. The first explanation is overestimation of the metric when a larger data range of two variables is compared (82). As PAT is the sum of PTT and PEP, when PTT and PEP change in the same direction, the change in PAT becomes larger than PTT and PEP, thus yielding higher correlation with SBP. This can explain the consistently higher correlation of SBP compared to that of DBP in both PTT and PAT in the cycling protocol (see Fig. 3.5), as SBP changes much more than DBP. Another possible explanation is that PEP can better respond to hemodynamic changes than PTT in a dynamic exercise such as cycling (40). As the dynamic exercise tends to increase SBP dominantly compared to DBP (66) , the change in PTT can also be restricted. On the contrary, a decrease in PEP can be consistent owing to the increased cardiac contractility that instantly responds to activation of the sympathetic nerve during exercise in general (83), which accordingly results in a consistent decrease in PAT. The higher standard deviation of change in PTT than that of change in PEP and PAT in exercise (see Table 3.2) can support this explanation.

Overall, the consistent correlation of PTT with BP compared to that of PAT in all protocols confirms the theory and previous

results (36, 38) and provides reliable tracking of BP in all cases. However, although PAT often shows better correlation with SBP, the use of PAT should be sublated since the inconsistent relationship of PAT with both BPs could estimate a change in BP in a different direction from the true BP.

In the pooled datasets, the correlation of PTT and PAT with BPs was approximately averaged between the two protocols, which was within a range similar to those reported in previous studies, such as −0.8 for PTT with SBP (34), −0.83 for PAT with SBP (63). −0.66–−0.8 for PTT with DBP (34, 38), and −0.4 ± 0.35 for PAT with DBP (84), where the correlation was computed in pooled datasets from multiple interventions. Note that the correlation of PAT with BPs ($r = -0.81$ and $r = -0.54$ for SBP and DBP) in the pooled dataset is relatively higher than those reported from previous studies. This may be attributed to the fact that a strong correlation in exercise is pronounced in the pooled dataset, as the change in BP in exercise was larger than that in the HDU protocol, which implies that depending on the types of intervention and the degree of changes in BP, the correlation of parameters with BP may vary. Therefore, the magnitude of correlation should be interpreted with caution,

considering the types of intervention and how datasets were pooled from each intervention.

In this study, a different change in PEP with PTT was found in the HDU protocol, whereas the previous study induced this phenomenon in cold-pressor intervention (34). However, in this study, though the detailed results are not included, when the cold pressor intervention was performed to induce BP changes, it seemed that not only the change in afterload was increased, but also the sympathetic nerve was activated depending on the subject. This may increase cardiac contractility, thereby resulting in frequent decrease in PEP and the failure in showing the degradation of PAT performance.

3.4.3. Enhancement of PTT based BP estimation

Although it is obvious that one variable cannot explain two independent targets, as SBP and DBP show a tight correlation in general, PTT has been serving as a common surrogate marker of both BPs in many previous studies. However, low correlation between SBP and DBP is often observed depending on the

situation, which was pronounced when a subject cycled in this study. Cycling is one of the dynamic exercises where SBP generally increases, whereas DBP remains unchanged, compared to the static exercise, which increases both BPs (66). During a dynamic exercise, the activated sympathetic nerve greatly increases HR and SV, and thus, CO, while TPR is generally decreased due to vascular dilation in the active muscle(66) in general. Depending on the subject and type of exercise, the proportion of increase in CO to decrease in TPR varies, which results in a relatively small increase in DBP or unchanged DBP, as DBP is closely affected by the combination of CO and TPR. On the contrary, the great increase in SBP is attributed to the increase in PP due to increased SV, which is mostly affected by cardiac ejection and arterial elastance. Thus, in the case when the change in SBP is dominant compared to that in DBP, the performance of BP estimation based on a change in PTT can be low owing to the fact that PTT is more associated with DBP, according to the theory, and that the change in PTT can be blurred by a measurement error when the change in DBP is narrow. As the low correlation between BPs can be attributable to the effect of PP, whose change is not based on the

conventional PTT–BP relationship, an independent indicator of PP may complement the BP estimation in particular cases.

In this study, we incorporated SA as an indicator of PP independent of PTT, thereby complementing the SBP estimation in conjunction with PTT (Fig. 3.6). The combination of PTT and SA allowed the improvement of the SBP estimation when a substantial change in SBP was induced compared to DBP by exercise, and thus provided independent tracking of SBP and DBP.

Additionally, the proposed model was compared with HR, which is one of popular hemodynamic parameters related with BP, as various time features in the bio-signals synchronized with heart beat have the possibility of being affected by HR. Figure 3. 16 shows the correlation of HR with BP in two interventions, along with that of the proposed model with BP. In cycling, HR increased along with BP, which resulted in a fair correlation, while HR exhibited almost no correlation with BP in the HDU protocol. In contrast, the proposed model showed a tight correlation with BPs in both interventions, which suggests that the proposed model

can track BP in the HR–BP coupled situation and in the decoupled situation.

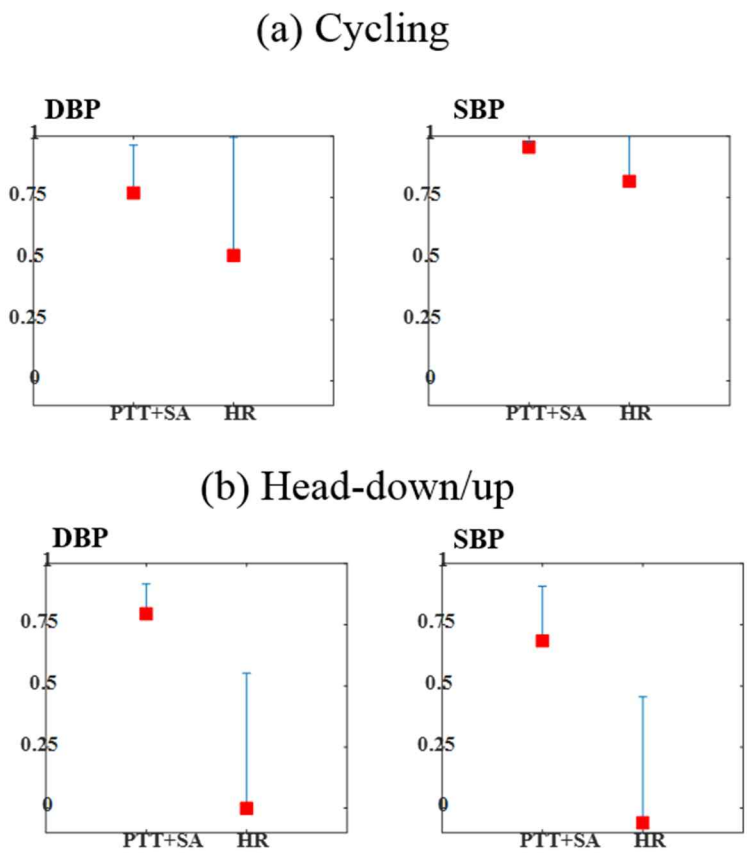

Figure 3.16 Correlation between HR–BPs and the proposed model–BPs in the (a) cycling protocol and the (b) HDU protocol.

As we guessed, it was found that SA was very well correlated with PP in the pooled datasets from different interventions ($r = 0.78 \pm 0.13$), and the correlation between the estimation by SA and reference PP was markedly high ($r = 0.91$, see Fig. 3.8) In the cycling protocol, when PP dominantly and greatly increases, the change in SA was prominent (see Fig. 3.4), resulting in high correlation between PP and SA. Accordingly, even in the case when PP was slightly decreased or unchanged in the HDU protocol, SA did not show change (see Fig. 3.4).

The relationship between SA and PP resides in the assumption that SA can reflect SV based on the genesis of SCG (43, 85). It is the recording of acceleration, which is directly generated by the force of cardiac vibration. Particularly, the first peak amplitude of SCG is mainly caused by the force of cardiac contraction as it appears in an isovolumetric contraction period when the heart contracts without volume change before the cardiac ejection commences, which determines the amount of blood ejected to the aorta or, in other words, SV. The main factors of SV are the blood volume in LV in the end-diastole period, and cardiac contractility, which is the innate ability of the heart muscle to change in force. According to the length-tension

relationship observed in the cardiac muscle, the increase in the blood volume in the LV in diastole stretches the cardiac muscle fibers, resulting in an increase in the force of cardiac contraction (86). Besides, when cardiac contractility increases, the force of cardiac contraction obviously increases accordingly, which physiologically backs up the assumption.

Some other features in SCG have also potential to track SV, such as PEP, and the time delay between the AO point and the aortic valve closing point (AC) in SCG, which is known as the left-ventricle ejection time (LVET) (44). However, PEP requires measurement of an additional bio-signal, ECG, which might lower the stability of the system as more types of signal measurements are required. Although ECG is being measured in the current design of the system for the purpose of comparison with the reference PEP and robust signal processing, this could be excluded in a future version, which will render the system more simple and compact (the width of the device was set in the current dimension owing to the minimal distance of the two electrodes) with an improved signal processing technique using SCG AO peak gating instead of ECG R-peak gating. When PEP and SA were compared in terms of correlation between the

calibrated and reference PP, this study found that the correlation of SA with PP was slightly higher than that of PP in pooled datasets from two interventions (r = 0.91 and 0.90 for SA and PEP, respectively), which supports the advantage of using SA over PEP in the current design of the system. On the other hand, LVET, although substantially associated with SV, was difficult to be extracted from the SCG waveform, as the detection of the second peak of SCG was hardly available, especially in conditions where movements were accompanied, which may reduce the practicality of the system.

3.4.4. Generalization

The principle of PTT–BP relationship is subject-dependent as the equations describing the relationship between PTT and arterial elastance and between BP and arterial elastance depend on subject-specific parameters, such as the property of the blood vessel wall, which varies by person. Thus, the majority

of the presented works using the PTT–BP relationship have shown their performance using a subject–dependent calibration, which calibrated the model to the reference BP for each subject. However, this process generally requires BP changes and measurements of BP and surrogate markers of BP during the BP changes, at least twice or more depending on the complexity of the model to derive the proportion of changes of the surrogate markers of BP to changes of BP for each subject, which is quite impractical and burdens a user. In order to alleviate the difficulty of the calibration process, we pre–determined the coefficients of variates by using a modified least square method, which requires only one single measurement of BPs and the parameters within 1 min, to apply it on a new subject. We derived the pre–determined model, tested the model for the datasets of different subject groups, and found that the group model could be applied to new subject group, which was even larger than the subject group from which the model was derived, with a fairly small error range. It is very appreciable that the performance satisfied the IEEE standard, even though the pre–determined model was applied to new subjects with just an additional single measurement for individual calibration, which suggests that the

proposed model using PTT and SA has the potential to be generalized and may simplify the calibration process.

3.4.5. BP monitoring in daily life

The conventional BP measurement, usually conducted in clinics by cuff, has been criticized for the fact that it cannot provide an accurate BP status of a subject owing to many reasons, including the variability of BP (18) and terminal digit preferences (87, 88). In addition, the prevalence of the white-coat syndrome, which masks the real BP status and may lead to a misdiagnose of hypertension, can be as high as 30% (89). Therefore, numerous studies have demonstrated the importance of 24-h ABPM (65, 87, 90–98), which can not only exclude the white-coat hypertension but also provide independent clinical values, pointing out that ABPM is a better predictor of morbidity than the conventional BP measurements in clinics (90–97). Furthermore, the circadian change of BP during a day has attracted wide attention since the nocturnal drop of BP, called dipping, was

found to be a strong risk indicator of cardiovascular disease in such way that a diminished nocturnal BP decline can be associated with higher risk of cardiovascular events (93, 99–103). However, the current cuff-type devices providing ABPM are limited to their use by particular subjects who already have been diagnosed in a clinic and are paying attention to their BP status owing to its highly discomforting aspect, especially during sleep. The results of the study by the proposed system design and model can provide ABPM more continuously than the conventional cuff-type ABPM, which is limited to use with intervals as short as approximately 15 min (65) without any requirement of a subject to intervene. Furthermore, as Fig. 3.14 demonstrates, this system can provide a way to assess the nocturnal drop without the discomfort of inflating and deflating a cuff, which could not be achieved by other recent studies of cuffless BP monitoring that require the subject to behave in a particular posture such as standing or sitting on a specialized apparatus (31, 38) and touching on a device with the finger-tip (104–106). Therefore, the proposed system could expand the use of ABPM not only for subjects who are already on the risk

of cardiovascular disease, but also for pre-hypertensive and normotensive subjects.

3.4.6. Limitation and future work

This study has a few limitations that should be addressed in a future study.

Firstly, the model validation was conducted only in a limited population of young and healthy male subjects. A future study should validate the proposed model against a more diverse population, including hypertensive and female subjects. It should be noted that, in the generalization, we derived the group model from subjects who are young and heathy, and applied it to those who can be regarded as homogeneous with the model-derived subject population. As the characteristic of the blood vessel wall could have homogeneity between subjects having similar vascular properties, the difference in the PTT–BP relationship can be prominent between normotensive and hypertensive subjects (107–109) and one's BP status could alter the PTT–BP

relationship. Thus, this group model may not be applicable to a different population, with subjects who are relatively older and hypertensive. Yet, as the young and normotensive subjects are those who lack compliance to daily BP monitoring and are mostly ignorant of their BP status, this convenient calibration process could increase the participation of this population into daily BP monitoring. This could allow early detection of their possible unwitting deterioration of the BP status, which otherwise could have not been detected. Secondly, the reference BP measurement may pose some limitations in the daily BP monitoring. Cuff-based BP measurement is influenced by the relative position of the arm with respect to the heart level. In other words, if the arm position is not aligned with the heart level, the measured BP is a sum of BP itself and hydrostatic pressure, depending on the height difference between arm and heart. In daily monitoring, especially during sleep, the arm position cannot be controlled, and thus, the relative position between arm and heart can be altered, which might result in an unreliable reference BP measurement. Moreover, when measuring the reference BP with an oscillometric BP measurement device, it is required that the subjects be in stable position when the

reference BP is measured, which might prevent from observing the dynamic BP variation in daily life. Thirdly, the relationship between SA and SV should be more carefully validated with the reference SV in various circumstances, given that it is a ground for SA to become an indicator of PP. Although SA has a potential to reflect the cardiac ejection force, which is likely to reflect a possible change in SV determinants, the direct relationship between SA and SV should be further studied.

CHAPTER 4

CONCLUSION

4.1. THESIS SUMMARY AND CONTRIBUTIONS

A single wearable device that can truly measure the PTT using SCG and PPG was developed along with a data acquisition program in dual platforms. Multi-channels of PPG, equipped with a feedback loop preventing saturation by a DC offset of PPG, were developed to increase the SNR of PPG in the chest, which enables a stable acquisition of the PPG waveform, and thus, the calculation of PTT with SCG. Also, the power consumption of PPG, which accounts for a large portion of that of the whole system, was dramatically cut by implementing a specialized LED dimming scheme, which allowed the system to operate for 24 h. This realized continuous and long-term monitoring in daily life. Furthermore, by the experiments, the repeatability of BP-related parameters was verified, which showed that the parameters, including SA, were not excessively affected by the fashion of wearing the device. Lastly, the reference PEP and the device-derived PEP were compared, providing evidence of the equivalence between two PEPs, even under wide hemodynamic changes. This implies in turn that the true PTT is obtained by the developed system.

The current limitation of the PTT–BP relationship was analyzed by the contrastive experiment, and the proposed model was compared with conventional models using PTT or PAT in two contrary interventions. Furthermore, the proposed model was generalized to new subjects and the potential of real use of the system was demonstrated in daily life. The results showed that (1) the proposed model, which employed SA in conjunction with PTT for SBP estimation, outperformed the conventional univariate model using PTT or PAT, and therefore, enabled independent estimation of SBP and DBP, which can often show different movements; (2) for practical use, the proposed model showed the potential to be generalized beyond a subject-dependent model fitting; and (3) the proposed model and system demonstrated the potential of continuous BP monitoring in daily life, including during sleep, with just a simple calibration and without any intervention of users or regulations.

In conclusion, the developed wearable system will facilitate continuous BP monitoring in daily life, including sleep period, with enhanced PTT based BP modeling, hence providing a more reliable assessment of the BP status and creating the opportunity to predict and prevent cardiovascular events in an early stage

4.2. FUTURE DIRECTION

The developed wearable system providing cuffless BP monitoring based on the PTT–BP relationship can be further enhanced in some aspects. In terms of system design, the current system can still be a burden to the user as it requires a strap band around the upper body to firmly establish contact with the chest skin. This can be solved by transforming the current design of the system into a stand−alone patch−type device, which can be readily attached to and detached from the body and, at the same time, retain the stable contact with the chest skin. Additionally, the power consumption can be lowered by applying an advanced power management algorithm which turns on/off the whole system by monitoring the activity of the user. For example, if the system automatically detects certain circumstances and turns off the device, when the subject engages in excessive movements, such as running, climbing, and weight training, where signal instrumentation is hardly available, an additional reduction of power consumption can be obtained. Furthermore, benefiting from the sampling method, it can be sufficient to measure the signals on an occasional basis, such as 30 s of

measurement every 5 or 10 min. This procedure still involves higher frequency than that of the conventional cuff-type ABPM and is able to reduce the power consumption by 80–90%. This kind of methods will provide the opportunity to use a smaller battery, which can, in turn, reduce the weight of the system, thereby increasing the contact and signal quality of the device.

On the other hand, the proposed model should be validated against a more diverse population of hypertensive and female subjects to reinforce the efficacy of the model. Further, the relationship between SA and SV, or SA and PP, should be more carefully assessed in various circumstances as the direct relationship between SA and SV is not yet well understood. Furthermore, as SCG contains rich information of cardiac movements, including timing of the second valve closing and the concomitant peak amplitude when the aortic valve closes, which is also known to be associated with BP (110), additional features can complement the model based on the PTT–BP relationship, thus increasing its performance.

BIBLIOGRAPHY

1. Gupta B. Invasive blood pressure monitoring. Update in Anaethesia. 2012;28:37−42.
2. Chen Y, Wen C, Tao G, Bi M, Li G. Continuous and noninvasive blood pressure measurement: a novel modeling methodology of the relationship between blood pressure and pulse wave velocity. Annals of biomedical engineering. 2009;37(11):2222−33.
3. Avolio AP, Butlin M, Walsh A. Arterial blood pressure measurement and pulse wave analysis−−their role in enhancing cardiovascular assessment. Physiological measurement. 2010;31(1):R1−47.
4. al. BPMIe. Fifteen years experience with finger arterial pressure monitoring: assessment of the technology. Cardiovasucular Research. 1998;38:605~16.
5. Kearney PM, Whelton M, Reynolds K, Muntner P, Whelton PK, He J. Global burden of hypertension: analysis of worldwide data. The lancet. 2005;365(9455):217−23.
6. Hernandorena I, Duron E, Vidal J−S, Hanon O. Treatment options and considerations for hypertensive patients to prevent dementia. Expert opinion on pharmacotherapy. 2017;18(10):989−1000.
7. Lackland DT, Weber MA. Global burden of cardiovascular disease and stroke: hypertension at the core. Canadian Journal of Cardiology. 2015;31(5):569−71.
8. Lau DH, Nattel S, Kalman JM, Sanders P. Modifiable risk factors and atrial fibrillation. Circulation. 2017;136(6):583−96.
9. Mendis S, Puska P, Norrving B. Global atlas on cardiovascular disease prevention and control: World Health Organization; 2011.
10. Burt VL, Whelton P, Roccella EJ, Brown C, Cutler JA, Higgins M, et al. Prevalence of Hypertension in the US Adult Population. Results From the Third National Health and Nutrition Examination Survey, 1988−1991. 1995;25(3):305−13.
11. Whelton PK. Epidemiology of hypertension. The Lancet. 1994;344(8915):101−6.
12. Whelton PK, Perneger TV, Brancati FL, Klag MJ. Epidemiology and prevention of blood pressure−related renal disease. Journal of Hypertension. 1992;10:S85.

13. Pickering TG, Miller NH, Ogedegbe G, Krakoff LR, Artinian NT, Goff D. Call to action on use and reimbursement for home blood pressure monitoring: a joint scientific statement from the American Heart Association, American Society of Hypertension, and Preventive Cardiovascular Nurses Association. Hypertension. 2008;52(1):10-29.
14. Atkins N, O'Brien E, Wesseling KH, Guelen I. Increasing observer objectivity with audio-visual technology: the Sphygmocorder. Blood pressure monitoring. 1997;2(5):269-72.
15. Williams B, Poulter N, Brown M, Davis M, McInnes G, Potter J, et al. Guidelines for management of hypertension: report of the fourth working party of the British Hypertension Society, 2004—BHS IV. Journal of human hypertension. 2004;18(3):139.
16. Mancia G, Parati G. The role of blood pressure variability in end-organ damage. Journal of hypertension. 2003;21:S17-S23.
17. Peixoto A, White W. Circadian blood pressure: clinical implications based on the pathophysiology of its variability. Kidney international. 2007;71(9):855-60.
18. Pickering TG, Harshfield GA, Devereux RB, Laragh JH. What is the role of ambulatory blood pressure monitoring in the management of hypertensive patients? Hypertension. 1985;7(2):171-7.
19. Pickering TG, Davidson K, Gerin W, Schwartz JE. Masked hypertension. Hypertension. 2002;40(6):795-6.
20. McDonald DA. Blood flow in arteries. 1974.
21. Korteweg D. Ueber die Fortpflanzungsgeschwindigkeit des Schalles in elastischen Röhren. Annalen der Physik. 1878;241(12):525-42.
22. Moens A. Over de voortplantingssnelheid von den pols (On the speed of propagation of the pulse). Acad Profsch, Leiden. 1877;1:1-72.
23. Moens A. Die Pulskurve [the Pulse Curve]. Leiden, The Netherlands. 1878.
24. Milnor W. Hemodynamics (Baltimore, MD: Williams and Wilkins). 1982.
25. Hughes D, Babbs CF, Geddes L, Bourland J. Measurements of Young's modulus of elasticity of the canine aorta with ultrasound. Ultrasonic Imaging. 1979;1(4):356-67.
26. Mukkamala R, Hahn J-O, Inan OT, Mestha LK, Kim C-S, Toreyin H, et al. Toward ubiquitous blood pressure monitoring

via pulse transit time: theory and practice. IEEE Trans Biomed Engineering. 2015;62(8):1879-901.
27. Cattivelli FS, Garudadri H, editors. Noninvasive cuffless estimation of blood pressure from pulse arrival time and heart rate with adaptive calibration. Wearable and Implantable Body Sensor Networks, 2009 BSN 2009 Sixth International Workshop on; 2009: IEEE.
28. Chen W, Kobayashi T, Ichikawa S, Takeuchi Y, Togawa T. Continuous estimation of systolic blood pressure using the pulse arrival time and intermittent calibration. Medical and Biological Engineering and Computing. 2000;38(5):569-74.
29. Geddes L, Voelz M, James S, Reiner D. Pulse arrival time as a method of obtaining systolic and diastolic blood pressure indirectly. Medical and Biological Engineering and Computing. 1981;19(5):671-2.
30. Muehlsteff J, Aubert X, Morren G, editors. Continuous cuff-less blood pressure monitoring based on the pulse arrival time approach: The impact of posture. Engineering in Medicine and Biology Society, 2008 EMBS 2008 30th Annual International Conference of the IEEE; 2008: IEEE.
31. Tang Z, Tamura T, Sekine M, Huang M, Chen W, Yoshida M, et al. A Chair-Based Unobtrusive Cuffless Blood Pressure Monitoring System Based on Pulse Arrival Time. IEEE journal of biomedical and health informatics. 2017;21(5):1194-205.
32. Ding X, Yan BP, Zhang Y-T, Liu J, Zhao N, Tsang HK. Pulse transit time based continuous cuffless blood pressure estimation: A new extension and a comprehensive evaluation. Scientific reports. 2017;7(1):11554.
33. Zhang G, Gao M, Xu D, Olivier NB, Mukkamala R. Pulse arrival time is not an adequate surrogate for pulse transit time as a marker of blood pressure. Journal of applied physiology. 2011;111(6):1681-6.
34. Martin SL-O, Carek AM, Kim C-S, Ashouri H, Inan OT, Hahn J-O, et al. Weighing scale-based pulse transit time is a superior marker of blood pressure than conventional pulse arrival time. Scientific reports. 2016;6:39273.
35. Foo JYA, Lim CS. Dual-channel photoplethysmography to monitor local changes in vascular stiffness. Journal of clinical monitoring and computing. 2006;20(3):221-7.
36. Payne R, Symeonides C, Webb D, Maxwell S. Pulse transit time measured from the ECG: an unreliable marker of beat-to-beat blood pressure. Journal of Applied Physiology.

2006;100(1):136-41.
37. Sola J, Proença M, Ferrario D, Porchet J-A, Falhi A, Grossenbacher O, et al. Noninvasive and nonocclusive blood pressure estimation via a chest sensor. IEEE Transactions on Biomedical Engineering. 2013;60(12):3505-13.
38. Kim C-S, Carek AM, Mukkamala R, Inan OT, Hahn J-O. Ballistocardiogram as proximal timing reference for pulse transit time measurement: Potential for cuffless blood pressure monitoring. IEEE Transactions on Biomedical Engineering. 2015;62(11):2657-64.
39. Nürnberger J, Dammer S, Saez AO, Philipp T, Schäfers R. Diastolic blood pressure is an important determinant of augmentation index and pulse wave velocity in young, healthy males. Journal of human hypertension. 2003;17(3):153.
40. Muehlsteff J, Aubert X, Schuett M, editors. Cuffless estimation of systolic blood pressure for short effort bicycle tests: the prominent role of the pre-ejection period. Engineering in Medicine and Biology Society, 2006 EMBS'06 28th Annual International Conference of the IEEE; 2006: IEEE.
41. Tavakolian K. Characterization and analysis of seismocardiogram for estimation of hemodynamic parameters: Applied Science: School of Engineering Science; 2010.
42. Crow RS, Hannan P, Jacobs D, Hedquist L, Salerno DM. Relationship between seismocardiogram and echocardiogram for events in the cardiac cycle. American journal of noninvasive cardiology. 1994;8:39-46.
43. Di Rienzo M, Vaini E, Castiglioni P, Merati G, Meriggi P, Parati G, et al. Wearable seismocardiography: Towards a beat-by-beat assessment of cardiac mechanics in ambulant subjects. Autonomic Neuroscience. 2013;178(1-2):50-9.
44. Tavakolian K, Blaber AP, Ngai B, Kaminska B, editors. Estimation of hemodynamic parameters from seismocardiogram. Computing in Cardiology, 2010; 2010: IEEE.
45. Zanetti JM, Tavakolian K, editors. Seismocardiography: Past, present and future. Engineering in Medicine and Biology Society (EMBC), 2013 35th Annual International Conference of the IEEE; 2013: IEEE.
46. Gaddum N, Alastruey J, Beerbaum P, Chowienczyk P, Schaeffter T. A technical assessment of pulse wave velocity algorithms applied to non-invasive arterial waveforms. Annals of biomedical engineering. 2013;41(12):2617-29.
47. Tavakolian K, Blaber AP, Ngai B, Kaminska B, editors.

Estimation of hemodynamic parameters from seismocardiogram. 2010 Computing in Cardiology; 2010 26-29 Sept. 2010.
48. Kannel WB, Gordon T, Schwartz MJ. Systolic versus diastolic blood pressure and risk of coronary heart disease: the Framingham study. American Journal of Cardiology. 1971;27(4):335-46.
49. Gavish B, Ben-Dov IZ, Bursztyn M. Linear relationship between systolic and diastolic blood pressure monitored over 24 h: assessment and correlates. Journal of hypertension. 2008;26(2):199-209.
50. Sola J, Rimoldi SF, Allemann Y. Ambulatory monitoring of the cardiovascular system: the role of pulse wave velocity. New Developments in Biomedical Engineering: InTech; 2010.
51. Blacher J, Staessen JA, Girerd X, Gasowski J, Thijs L, Liu L, et al. Pulse pressure not mean pressure determines cardiovascular risk in older hypertensive patients. Archives of internal medicine. 2000;160(8):1085-9.
52. Dart AM, Kingwell BA. Pulse pressure—a review of mechanisms and clinical relevance. Journal of the American College of Cardiology. 2001;37(4):975-84.
53. Bombardini T, Gemignani V, Bianchini E, Venneri L, Petersen C, Pasanisi E, et al. Cardiac reflections and natural vibrations: Force-frequency relation recording system in the stress echo lab. Cardiovascular Ultrasound. 2007;5(1):42.
54. Korzeniowska-Kubacka I, Bilińska M, Piotrowicz R. Usefulness of seismocardiography for the diagnosis of ischemia in patients with coronary artery disease. Annals of noninvasive electrocardiology. 2005;10(3):281-7.
55. Gemignani V, Bianchini E, Faita F, Giannoni M, Pasanisi E, Picano E, et al., editors. Operator-independent force-frequency relation monitoring during stress with a new transcutaneous cardiac force sensor. Computers in Cardiology, 2007; 2007: IEEE.
56. Bombardini T, Gemignani V, Bianchini E, Venneri L, Petersen C, Pasanisi E, et al. Diastolic time–frequency relation in the stress echo lab: filling timing and flow at different heart rates. Cardiovascular ultrasound. 2008;6(1):15.
57. Steptoe A, Smulyan H, Gribbin B. Pulse wave velocity and blood pressure change: calibration and applications. Psychophysiology. 1976;13(5):488-93.
58. Gribbin B, Steptoe A, Sleight P. Pulse wave velocity as a measure of blood pressure change. Psychophysiology.

1976;13(1):86-90.
59. Remington JW, Noback CR, Hamilton W, Gold JJ. Volume elasticity characteristics of the human aorta and prediction of the stroke volume from the pressure pulse. American Journal of Physiology-Legacy Content. 1948;153(2):298-308.
60. Ferguson J, Julius S, Randall O. Stroke volume--pulse pressure relationships in borderline hypertension: a possible indicator of decreased arterial compliance. Journal of hypertension Supplement: official journal of the International Society of Hypertension. 1984;2(3):S397-9.
61. Randall O, Westerhof N, Alexander B. Reliability of stroke volume to pulse pressure ratio for estimating and detecting changes in arterial compliance. Journal of hypertension Supplement: official journal of the International Society of Hypertension. 1986;4(5):S293-6.
62. Froelicher VF, Myers J, Follansbee W, Labovitz A. Exercise and the Heart: WB Saunders Philadelphia; 2000.
63. Gesche H, Grosskurth D, Küchler G, Patzak A. Continuous blood pressure measurement by using the pulse transit time: comparison to a cuff-based method. European journal of applied physiology. 2012;112(1):309-15.
64. Masè M, Mattei W, Cucino R, Faes L, Nollo G. Feasibility of cuff-free measurement of systolic and diastolic arterial blood pressure. Journal of electrocardiology. 2011;44(2):201-7.
65. Lopez G, Shuzo M, Ushida H, Hidaka K, Yanagimoto S, Imai Y, et al. Continuous blood pressure monitoring in daily life. Journal of Advanced Mechanical Design, Systems, and Manufacturing. 2010;4(1):179-86.
66. Bezucha GR, Lenser M, Hanson P, Nagle F. Comparison of hemodynamic responses to static and dynamic exercise. Journal of Applied Physiology. 1982;53(6):1589-93.
67. Patel K, Rössler A, Lackner HK, Trozic I, Laing C, Lorr D, et al. Effect of postural changes on cardiovascular parameters across gender. Medicine. 2016;95(28).
68. McCrory C, Berkman LF, Nolan H, O'leary N, Foley M, Kenny RA. Speed of heart rate recovery in response to orthostatic challenge. Circulation research. 2016;119(5):666-75.
69. Zambrano SS, Spodick DH. Comparative responses to orthostatic stress in normal and abnormal subjects: evaluation by impedance cardiography. Chest. 1974;65(4):394-6.
70. Cooper V, Hainsworth R. Effects of head-up tilting on

baroreceptor control in subjects with different tolerances to orthostatic stress. Clinical Science. 2002;103(3):221-6.
71. Reulecke S, Charleston-Villalobos S, Voss A, González-Camarena R, González-Hermosillo J, Gaitan-Gonzalez MJ, et al. Orthostatic stress causes immediately increased blood pressure variability in women with vasovagal syncope. Computer methods and programs in biomedicine. 2016;127:185-96.
72. Suzuki J, Nakamura T, Hirayama M, Mizutani Y, Okada A, Ito M, et al. Impaired peripheral vasoconstrictor response to orthostatic stress in patients with multiple system atrophy. Parkinsonism & related disorders. 2015;21(8):917-22.
73. American National Standard for Electronic or Automated sphygmomanometers.: ANSI/AAMI SP; 10-1992. p. 40.
74. O'brien E, Petrie J, Littler W, Padfield P, O'Malley K, Jamieson M, et al. The British Hypertension Society protocol for the evaluation of automated and semi-automated blood pressure measuring devices with special reference to ambulatory systems. Journal of hypertension. 1990;8(7):607-19.
75. ASSOCIATION IS. IEEE STARDARD for Wearable, Cuffless Blood Pressure Measuring Devices. 2014.
76. Inan OT, Park D, Giovangrandi L, Kovacs GT. Noninvasive measurement of physiological signals on a modified home bathroom scale. IEEE Transactions on Biomedical Engineering. 2012;59(8):2137-43.
77. Krohová J, Czippelová B, Turianiková Z, Lazarová Z, Tonhajzerová I, Javorka M. Preejection period as a sympathetic activity index: a role of confounding factors. 2017.
78. Gao M, Olivier NB, Mukkamala R. Comparison of noninvasive pulse transit time estimates as markers of blood pressure using invasive pulse transit time measurements as a reference. Physiological reports. 2016;4(10):e12768.
79. Wong MY-M, Poon CC-Y, Zhang Y-T. An evaluation of the cuffless blood pressure estimation based on pulse transit time technique: a half year study on normotensive subjects. Cardiovascular Engineering. 2009;9(1):32-8.
80. Ahlstrom C, Johansson A, Uhlin F, Länne T, Ask P. Noninvasive investigation of blood pressure changes using the pulse wave transit time: a novel approach in the monitoring of hemodialysis patients. Journal of Artificial Organs. 2005;8(3):192-7.
81. Yoon Y, Cho JH, Yoon G. Non-constrained blood pressure monitoring using ECG and PPG for personal healthcare.

Journal of medical systems. 2009;33(4):261-6.
82. Laurent S, Cockcroft J, Van Bortel L, Boutouyrie P, Giannattasio C, Hayoz D, et al. Expert consensus document on arterial stiffness: methodological issues and clinical applications. European heart journal. 2006;27(21):2588-605.
83. Larkin KT, Kasprowicz AL. Validation of a simple method of assessing cardiac preejection period: A potential index of sympathetic nervous system activity. Perceptual and motor skills. 1986;63(1):295-302.
84. Lane JD, Greenstadt L, Shapiro D, Rubinstein E. Pulse transit time and blood pressure: an intensive analysis. Psychophysiology. 1983;20(1):45-9.
85. Tavakolian K, Ngai B, Akhbardeh A, Kaminska B, Blaber A, editors. Comparative analysis of infrasonic cardiac signals. Computers in Cardiology, 2009; 2009: IEEE.
86. Klabunde R. Cardiovascular physiology concepts: Lippincott Williams & Wilkins; 2011.
87. O'brien E. Ambulatory blood pressure measurement is indispensable to good clinical practice. Journal of Hypertension. 2003;21:S11-S8.
88. Keary L, Atkins N, Molloy E, Mee F, O'Brien E. Terminal digit preference and heaping in blood pressure measurement. J Hum Hypertens. 1998;12:787-8.
89. Pickering TG, James GD, Boddie C, Harshfield GA, Blank S, Laragh JH. How common is white coat hypertension? Jama. 1988;259(2):225-8.
90. Dolan E, Stanton A, Thijs L, Hinedi K, Atkins N, McClory S, et al. Superiority of ambulatory over clinic blood pressure measurement in predicting mortality: the Dublin outcome study. Hypertension. 2005;46(1):156-61.
91. Perloff D, Sokolow M, Cowan R. The prognostic value of ambulatory blood pressures. Jama. 1983;249(20):2792-8.
92. Redon J, Campos C, Narciso ML, Rodicio JL, Pascual JM, Ruilope LM. Prognostic value of ambulatory blood pressure monitoring in refractory hypertension: a prospective study. Hypertension. 1998;31(2):712-8.
93. Staessen JA, Thijs L, Fagard R, O'brien ET, Clement D, De Leeuw PW, et al. Predicting cardiovascular risk using conventional vs ambulatory blood pressure in older patients with systolic hypertension. Jama. 1999;282(6):539-46.
94. Ohkubo T, Imai Y, Tsuji I, Nagai K, Watanabe N, Minami N, et al. Prediction of mortality by ambulatory blood pressure

monitoring versus screening blood pressure measurements: a pilot study in Ohasama. Journal of hypertension. 1997;15(4):357-64.
95. Ohkubo T, Hozawa A, Nagaie K, Kikuya M, Tsujia I, Itoc S, et al. Prediction of stroke by ambulatory blood pressure monitoring versus screening blood pressure measurements in a general population: the Ohasama study. Journal of hypertension. 2000;18(7):847-54.
96. Clement D, De Buyzere M, De Bacquer D, De Leeuw P, Duprez D, Fagard R, et al. Office vs. Ambulatory Pressure Study Investigators. Prognostic value of ambulatory blood-pressure recordings in patients with treated hypertension. N Engl J Med. 2003;348:2407-15.
97. Verdecchia P, Schillaci G, Borgioni C, Ciucci A, Pede S, Porcellati C. Ambulatory pulse pressure: a potent predictor of total cardiovascular risk in hypertension. Hypertension. 1998;32(6):983-8.
98. Pickering TG, James GD. Ambulatory blood pressure and prognosis. Journal of hypertension Supplement: official journal of the International Society of Hypertension. 1994;12(8):S29-33.
99. Ohkubo T, Hozawa A, Yamaguchi J, Kikuya M, Ohmori K, Michimata M, et al. Prognostic significance of the nocturnal decline in blood pressure in individuals with and without high 24-h blood pressure: the Ohasama study. Journal of hypertension. 2002;20(11):2183-9.
100. Stolarz K, Staessen JA, T O'Brien E. Night-time blood pressure: dipping into the future? Journal of hypertension. 2002;20(11):2131-3.
101. Verdecchia P, Porcellati C, Schillaci G, Borgioni C, Ciucci A, Battistelli M, et al. Ambulatory blood pressure. An independent predictor of prognosis in essential hypertension. Hypertension. 1994;24(6):793-801.
102. Kario K, Pickering TG, Matsuo T, Hoshide S, Schwartz JE, Shimada K. Stroke prognosis and abnormal nocturnal blood pressure falls in older hypertensives. Hypertension. 2001;38(4):852-7.
103. Cuspidi C, Meani S, Salerno M, Valerio C, Fusi V, Severgnini B, et al. Cardiovascular target organ damage in essential hypertensives with or without reproducible nocturnal fall in blood pressure. Journal of hypertension. 2004;22(2):273-80.
104. Watanabe N, Bando YK, Kawachi T, Yamakita H,

Futatsuyama K, Honda Y, et al. Development and Validation of a Novel Cuff-Less Blood Pressure Monitoring Device. JACC: Basic to Translational Science. 2017;2(6):631-42.
105. Chandrasekhar A, Kim C-S, Naji M, Natarajan K, Hahn J-O, Mukkamala R. Smartphone-based blood pressure monitoring via the oscillometric finger-pressing method. Science translational medicine. 2018;10(431):eaap8674.
106. Matsumura K, Rolfe P, Toda S, Yamakoshi T. Cuffless blood pressure estimation using only a smartphone. Scientific reports. 2018;8(1):7298.
107. Gaddum NR, Keehn L, Guilcher A, Gomez A, Brett S, Beerbaum P, et al. Altered dependence of aortic pulse wave velocity on transmural pressure in hypertension revealing structural change in the aortic wall. Hypertension. 2015;65(2):362-9.
108. Ng K, Butlin M, Avolio AP. Persistent effect of early, brief angiotensin-converting enzyme inhibition on segmental pressure dependency of aortic stiffness in spontaneously hypertensive rats. Journal of hypertension. 2012;30(9):1782-90.
109. Butlin M, Shirbani F, Barin E, Tan I, Spronck B, Avolio A. Cuffless estimation of blood pressure: importance of variability in blood pressure dependence of arterial stiffness across individuals and measurement sites. IEEE Transactions on Biomedical Engineering. 2018.
110. Bombardini T, Gemignani V, Bianchini E, Venneri L, Petersen C, Pasanisi E, et al. Arterial pressure changes monitoring with a new precordial noninvasive sensor. Cardiovascular Ultrasound. 2008;6(1):41.

Abstract in Korean

국문 초록

커프리스 방식의 착용형 연속 혈압 모니터링 시스템에 관한 연구

고혈압의 조기 진단과 고혈압 환자의 혈압 관리를 위해서는 일상생활에서의 지속적인 혈압 모니터링이 중요하다. 맥파전달시간 (Pulse transit time, PTT) 기반의 혈압 추정 방식이 이를 가능케 하는 방법으로 가장 각광 받고 있지만, 맥파전달시간을 측정하기 위해서는 여러 측정 장치들이 필요하여 일상 생활에서의 사용에 제약이 있으며, 또한 맥파전달시간 만을 이용한 수축기 혈압(Systolic blood pressure, SBP) 추정 능력은 부족함이 있는 것으로 알려져 있다.

본 학위 논문의 첫 번째 목적은 맥파전달시간 측정 시스템을 착용형으로 개발하여 간편하게 맥파전달시간을 측정할 수 있도록 함으로써 일상 생활 중 맥파전달시간을 이용한 연속적인 혈압 모니터링이 가능케 하는 것이다. 이를 위해 광용적맥파 (Photoplethysmogram, PPG) 와 심진도 (Seismocardiogram,

SCG)를 동시에 측정하는 가슴 착용형 단일 장치를 개발하여, 심진도로부터 대동맥 판막의 열리는 시점을, 광용적맥파로부터 맥파의 도착 시점을 특정하여 맥파 전달 시간을 측정하였다. 개발된 시스템은 낮은 전력 소모와 소형의 간편한 디자인을 통해 24 시간 동안 연속적으로 사용할 수 있도록 설계되었다. 측정된 생체신호로부터 추출된 맥파전달시간 및 기타 혈압 관련 변수들이 기기의 반복 착용에도 변하지 않음을 급간내상관계수(Intra-class correlation, ICC) 분석을 통해 확인하였고 (ICC >0.8), 또한 본 시스템에서 사용된 심진도가 대동맥 판막의 열리는 시점의 레퍼런스가 될 수 있는지도 심저항신호(Impedancecardiogram, ICG)와의 비교를 통해 검증하였다(r=0.79±0.14).

둘째로, 개발된 시스템을 이용하여 기존의 맥파 전달 시간만을 이용한 혈압 추정 방식을 보완하여 수축기 혈압의 추정 능력이 향상된 알고리즘을 개발하였다. 이를 위해, 심진도의 진폭과 맥파 전달 시간을 같이 사용하는 다변수 모델을 수축기 혈압 추정을 위해 제안하였고, 다양한 방법으로 유도된 혈압 변화 상황에서, 기존의 맥파전달시간 혹은 맥파도달시간 (Pulse arrival time, PAT) 만을 이용한 모델과 그 성능을 비교하였다. 또한, 제안된 모델이 간단한 교정절차를 통해 여러 사람에게 적용될 수 있는 가능성을 살펴보았고 더 나아가 일상 생활에서의 사용 가능성에 대해서도 검증하였다. 그 결과로 제안된 모델은 (1) 기존의

맥파전달시간 혹은 맥파도달시간 만을 이용한 모델보다 수축기 혈압 추정 능력 측면에서 더 우수하였고, (각각의 평균절대오차는 4.57, 6.01, 6,11 mmHg 였다.) (2) 간단한 교정절차만을 통해서 여러 사람에게 적용 되었을 때의 추정 능력이 국제 기준에 부합하였으며, (3) 일상 생활에서도 사용자의 아무런 개입이나 제약 없이 지속적인 혈압 모니터링이 가능함을 확인하였다.

결론적으로 본 연구에서 제안하는 착용형 연속 혈압 측정 시스템은 가슴에 부착하는 단일 기기 형태로 그 사용이 간편할 뿐 아니라 일상생활 중에서 맥파전달시간과 심진도의 진폭을 이용하여 향상된 수준의 연속 혈압 모니터링 성능을 제공하였는바, 이를 이용한 모바일 헬스케어 서비스의 가능성을 확인하였다.

핵심어 : 혈압, 연속혈압 모니터링, 모바일헬스케어, 착용형 장치, 맥파전달시간, 광용적맥파, 심진도

학 번 : 2015-31046